

000 001 002 003 004 005 006 007 008 009 010 011 012 DUET: OPTIMIZING TRAINING DATA MIXTURES VIA COARSE, NOISY FEEDBACK FROM UNSEEN EVALUA- TION TASKS

013
014
015
016
017
018
019
020
021
022
023
024
025
026
027
028
029
030
031
032
033
034
035
036
037
038
039
040
041
042
043
044
045
046
047
048
049
050
051
052
053
Anonymous authors

Paper under double-blind review

ABSTRACT

The performance of an LLM depends heavily on the relevance of its training data to the downstream evaluation task. However, in practice, we do not have fine-grained knowledge of the data in the evaluation task (e.g., conversations between an LLM and a user are end-to-end encrypted). Hence, it is unclear what data is relevant for fine-tuning the LLM. Instead, we can only deploy the LLM on the unseen task to gather multiple rounds of coarse, noisy feedback on how well the model performs (e.g., user ratings). Our paper presents **DUET**, a novel global-to-local algorithm that optimizes training data mixtures by interleaving *data selection* with *Bayesian optimization* to exploit coarse and noisy feedback from a downstream evaluation task. DUET is flexible enough to incorporate different data selection methods, each with different performance-compute tradeoffs. By analyzing DUET’s *cumulative regret*, we theoretically show that DUET converges to the optimal training data mixture even without any fine-grained data information from an unseen task. Finally, our experiments across a variety of language tasks demonstrate that DUET attains substantial performance improvements over existing data selection and mixing methods in the unseen-task setting. Our anonymized code can be found at <https://github.com/pmsdapfmbf/DUET>.

1 INTRODUCTION

The performance of an LLM depends heavily on the composition of training data domains (Chen et al., 2024a; Xie et al., 2023a) and the downstream evaluation task (Hoffmann et al., 2022; Long et al., 2017). For instance, if we knew that LLM users are interested in asking layman science questions, then training or fine-tuning the LLM with more Wikipedia data allows it to converse better with these users. Hence, knowing the evaluation task is important for curating a more relevant training data mixture, producing an LLM with better performance over the specific task of interest.

However, in practice, the data (e.g., its domain, distribution, or labels) involved in an *unseen evaluation task* are often unknown. Thus, it is not obvious what data is relevant for training or fine-tuning the model. Instead, one can only deploy the LLM on the unseen evaluation task a few times to gather coarse feedback to see how well the model performs, creating a feedback loop. How can we efficiently use the (potentially noisy) feedback loop to improve and optimize the training data mixture? Consider the following problem setting: An LLM owner is interested in fine-tuning their LLM to converse better with users but due to privacy concerns (Li et al., 2024), conversations between the deployed LLM and users are end-to-end encrypted (openai.com/enterprise-privacy). Hence, the LLM owner does not know the actual evaluation data seen during test-time. Rather, we only receive coarse, noisy feedback on how well the LLM has performed in the conversation (e.g., user ratings or duration spent on the application) and gather multiple rounds of feedback from users.

This paper presents **DUET** (Fig. 1), a novel algorithm that exploits the feedback loop to optimize the training Data mixture for an Unseen Evaluation Task. DUET is a *global-to-local* algorithm that interleaves *data selection* (Albalak et al., 2024; Ting & Brochu, 2017; Koh & Liang, 2017) with *Bayesian optimization* (BO) (Snoek et al., 2012; Srinivas et al., 2010) to optimize the training data mixture. Globally, BO in DUET uses coarse, noisy feedback from the unseen evaluation task to automatically refine the mixing ratio of data domains in the training data mixture iteratively.

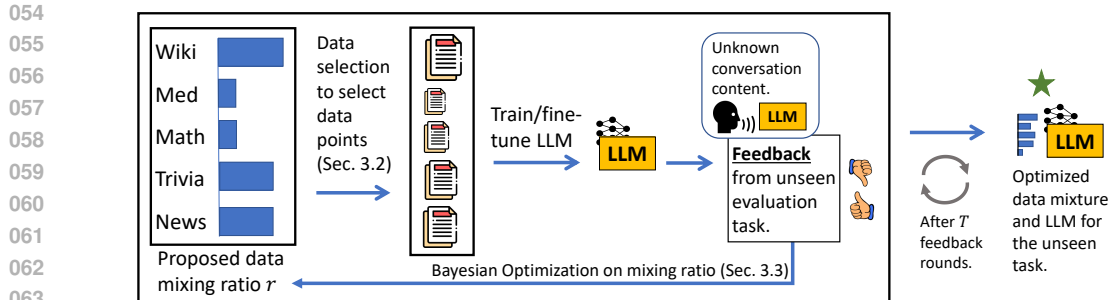


Figure 1: **DUET** exploits a feedback loop to optimize the data mixture for an unseen evaluation task. In contrast, conventional data mixing and selection works require fine-grained data information of the task, which is not available here.

Locally, DUET uses data selection to retrieve high-quality data points from each data domain until the proposed mixing ratio is reached. This results in an algorithm that can efficiently optimize training data even without having access to fine-grained data information from the evaluation task.

Related works. In our problem setting, (a) there is no direct access to the data (e.g., its domain, distribution, or labels) involved in the unseen evaluation task but (b) we can gather multiple rounds of feedback (details covered in Sec. 2.2) from the task using an LLM. App. A.1 provides a few more practical examples of this setting. This setting is different from those considered in conventional domain adaptation (DA) and domain generalization (DG) works. Prior DA works assume fine-grained knowledge of data (e.g., labeled/unlabeled data (Zhang et al., 2022) or data distribution (Ganin & Lempitsky, 2015; Zhang et al., 2021)) from the evaluation task for selecting relevant training data that match the evaluation data. On the other hand, DG considers a rigid setting with no knowledge (not even feedback) of the evaluation task (Muandet et al., 2013; Shin et al., 2024; Wang et al., 2022).

Similarly, *data mixing* works such as DoReMi (Xie et al., 2023a), BiMix (Ge et al., 2025) and more (Chen et al., 2024a; Fan et al., 2024; Xie et al., 2025; 2023b) introduced methods to optimize data mixtures, and *data selection* works (Albalak et al., 2024; Xia et al., 2024; Pruthi et al., 2020; Xie et al., 2023b) explored ways to find high-quality data to improve an LLM’s performance. However, these methods assume some availability of fine-grained evaluation data information, such as evaluation gradients, labels, distribution or naively assuming the training data shares the same distribution as the task. In practice (like in our setting), these are not always available. In fact, when we applied existing data mixing and selection methods directly to our setting, they perform worse than DUET (Sec. 6). We provide more discussion of the shortfalls of these prior works in App. A.2.

To the best of our knowledge, DUET is the first work that interleaves data selection with BO to iteratively optimize training data mixture based on feedback from an unseen evaluation task. At first glance, eliciting multiple rounds of feedback with BO seems expensive. However, BO is sample-efficient and is the only way we can exploit such coarse and noisy feedback iteratively, unlike prior methods that require much more fine-grained data information (see above). In fact, subjecting models to multiple rounds of training or fine-tuning in a feedback loop is a natural part of the deployment life-cycle to improve LLMs. Specifically, our contributions are:

- We introduce a novel and realistic problem setting where the data involved in an unseen evaluation task is unknown but we can deploy our LLM to gather multiple rounds of coarse and noisy feedback. Then, we introduce **DUET**, a novel algorithm that exploits the feedback loop to optimize training Data mixture for the Unseen Evaluation Task. To achieve this, DUET interleaves data selection (Sec. 3.2) with Bayesian optimization (Sec. 3.3) to iteratively optimize the training data mixture. DUET is flexible enough to incorporate any data selection choice in its inner loop, and we qualitatively and quantitatively analyzed different choices in our paper.
- We provide a theoretical analysis of DUET’s convergence to the optimal training data mixture by analyzing DUET’s *attained cumulative regret* (Chen et al., 2024b; Chowdhury & Gopalan, 2017) under the BO framework (Sec. 4).
- We demonstrate the effectiveness of DUET on LLM fine-tuning for language tasks comprising both in-domain and out-of-domain unseen tasks spanning different domains. Compared to conventional data selection and mixing methods (e.g., DoReMi, LESS, Aioli (Chen et al., 2024a) and more), DUET produces more optimal training data mixtures (Sec. 6.2).

108

2 PRELIMINARIES

109

2.1 BAYESIAN OPTIMIZATION

110 We first provide an outline of how BO can be used to optimize a generic black-box objective function
 111 before explaining how BO is used in DUET (Sec. 3.3). We consider a black-box objective function
 112 $f : \mathbb{R}^n \mapsto \mathbb{R}$ over the space of inputs $r \in \mathbb{R}^n$. As we show later (Sec. 2.2), we will use the data
 113 mixing ratio as r in our setting. The goal is to find $r^* \triangleq \arg \min_r f(r)$ which minimizes the objective
 114 function. BO is a query-efficient *active algorithm* that strategically selects input points to query
 115 the black-box objective function, conditioned on previous function observations. At each iteration
 116 $t = 1, 2, \dots, T$ of BO, we query the black-box function with a selected input r_t to obtain a *noisy*
 117 observation $\tilde{y}_t \triangleq f(r_t) + \epsilon_t$ with a sub-Gaussian noise ϵ_t (e.g., Gaussian or bounded noise) to form
 118 sample (r_t, \tilde{y}_t) . Consistent with (Chowdhury & Gopalan, 2017), we model the unknown function f
 119 as a realization of a *Gaussian process* (GP) (Williams & Rasmussen, 2006) that is fully specified by
 120 its *prior* mean $\mu(r)$ and covariance $\kappa(r, r')$ for all $r, r' \in \mathbb{R}^n$ where κ is a *kernel* function chosen
 121 to characterize the correlation of the observations between any two inputs r and r' ; a common
 122 choice is the *squared exponential* (SE) kernel $\kappa(r, r') \triangleq \exp(-\|r - r'\|_2^2/(2m^2))$ with a *length-scale*
 123 hyperparameter m that can be learned via maximum likelihood estimation. Given a column vector
 124 $\mathbf{y}_t \triangleq [\tilde{y}_\tau]_{\tau=1, \dots, t}^\top$ of noisy observations at previous inputs r_1, \dots, r_t , the posterior belief of f at any
 125 new input r' is a Gaussian distribution with the following *posterior* mean and variance:
 126

$$\begin{aligned} \mu_t(r') &\triangleq \kappa_t^\top(r')(K_t + \zeta I)^{-1}\mathbf{y}_t \\ \sigma_t(r') &\triangleq \kappa(r', r') - \kappa_t^\top(r')(K_t + \zeta I)^{-1}\kappa_t(r') \end{aligned} \quad (1)$$

127 where $\kappa_t(r') \triangleq [\kappa(r', r_\tau)]_{\tau=1, \dots, t}^\top$ is a column vector, $K_t \triangleq [\kappa(r_\tau, r_{\tau'})]_{\tau, \tau'=1, \dots, t}$ is a $t \times t$ covariance
 128 matrix, and $\zeta > 0$ is viewed as a free hyperparameter that depends on the problem setting (Chowdhury
 129 & Gopalan, 2017). Using equation 1, the BO algorithm selects the next input query r_{t+1} by optimizing
 130 an *acquisition function*, such as minimizing the *lower confidence bound* (LCB) acquisition function
 131 (Srinivas et al., 2010): $r_{t+1} = \arg \min_r \mu_t(r) - \beta_{t+1}\sigma_t(r)$ with an exploration parameter β_{t+1} . In
 132 addition, BO can also handle constraints on inputs r (Gardner et al., 2014). The cumulative regret
 133 (for T BO iterations w.r.t. a minimization problem) $R_T \triangleq \sum_{t=1}^T [f(r_t) - f(r^*)]$ is used to assess
 134 the performance of a BO algorithm (Tay et al., 2023) given that $f(r^*)$ is the true function minimum.
 135 A lower cumulative regret indicates a faster convergence rate. We provide a theoretical analysis of
 136 DUET's cumulative regret in Sec. 4.
 137

138

2.2 PROBLEM SETTING: OPTIMIZING DATA MIXTURES FOR AN UNSEEN TASK

139 Now, we formally describe our problem setting. Suppose that we have n training datasets $\mathcal{D} \triangleq$
 140 $\{D_1, D_2, \dots, D_n\}$ from n different domains (e.g., Wikipedia, ArXiv), where \mathcal{D} is the union of these
 141 training datasets. Let $\mathcal{L}_{\text{eval}}(\theta)$ be the unseen evaluation task loss w.r.t. an LLM parameterized by
 142 θ . This "loss" represents feedback from the unseen evaluation task and does not have a closed,
 143 mathematical form. Our goal is to find an optimal data mixture $\mathcal{X}^* \in \mathcal{D}$ (a set of training data points)
 144 and learn model parameters $\theta_{\mathcal{X}^*}$ such that the unseen evaluation task loss $\mathcal{L}_{\text{eval}}$ is minimized:
 145

$$\begin{aligned} \min_{\mathcal{X} \in \mathcal{D}} \quad & \mathcal{L}_{\text{eval}}(\theta_{\mathcal{X}}) \\ \text{s.t.} \quad & |\mathcal{X}| = M, \end{aligned} \quad (2)$$

146 where $\theta_{\mathcal{X}} \triangleq \arg \min_{\theta} \mathcal{L}_{\text{train}}(\mathcal{X}, \theta)$ is the model parameters learned in a standard supervised learning
 147 manner (e.g., gradient descent) from a chosen data mixture \mathcal{X} and $\mathcal{L}_{\text{train}}$ is a standard model training
 148 loss (e.g., cross-entropy loss for LLM prediction). To make our theoretical formulation and expository
 149 simpler, we consider the feedback $\mathcal{L}_{\text{eval}}$ deterministic. However, DUET works equally well for in
 150 noisy feedback setting, which we demonstrate empirically (Sec. 6) and elaborate in App. A.3. M is a
 151 practical, pre-decided constraint (Mirzasoleiman et al., 2020) to ensure the selected data mixture is
 152 not too large. In practice, evaluation task loss $\mathcal{L}_{\text{eval}}$ is just a feedback that indicates how well the LLM
 153 is performing and does not contain any evaluation data information. It can also be interchanged with
 154 other measures to be maximized (e.g., accuracy, user ratings) with slight mathematical adjustment to
 155 later statements.
 156

162 3 OPTIMIZING TRAINING DATA MIXTURES USING DUET 163

164 Unfortunately, solving problem 2 is challenging because the unseen evalua-
165 tion task loss $\mathcal{L}_{\text{eval}}$ does not have a closed, mathematical form and finding
166 the optimal data mixture \mathcal{X}^* directly is a high-dimensional discrete op-
167 timization problem. To address this, DUET adopts a global-to-local
168 approach to optimize the training data mixture. Globally, DUET uses
169 BO to adjust the mixing ratio in the data mixture adaptively based on
170 the task feedback. Locally, we interleave a data selection method of
171 choice (depending on the practitioner’s compute budget) to refine the data
172 mixture every iteration. Fig. 2 illustrates, in a simple setting, how DUET
173 progressively finds better data mixtures close to the optimal (green star).
174 We also discuss several extensions of DUET in App. A.3.

175 3.1 REPARAMETERIZATION OF THE OPTIMIZATION PROBLEM 176

177 We first reparameterize the objective function of problem 2 into a bilevel optimization problem that, at
178 the outer level, depends on the mixing ratio $r \in \mathbb{R}^n$ of training data domains (such reparameterization
179 has been considered in AutoML works (Chen et al., 2024b)). This reparameterized problem has a
180 unique structure that aligns with DUET’s global-to-local nature (Sec. 3.2 & 3.3).

181 **Theorem 3.1.** \mathcal{X}^* , the optimal set of data points from \mathcal{D} , is the solution of the original problem 2 iff
182 $r^* = \text{ratio}(\mathcal{X}^*)$ is the optimal mixing ratio solution of the reparameterized problem:

$$\min_{r \in \mathbb{R}^n} \min_{\mathcal{X} \in S_r} \mathcal{L}_{\text{eval}}(\theta_{\mathcal{X}}), \quad (3)$$

185 where $S_r \triangleq \{\mathcal{X} : \mathcal{X} \in \mathcal{D}, \text{ratio}(\mathcal{X}) = r, |\mathcal{X}| = M\}$ and $\text{ratio}(\mathcal{X}) = r$ means that the data points in
186 \mathcal{X} satisfies the mixing ratio $r \in \mathbb{R}^N$ from n data domains and $\|r\|_1 = 1$.
187

188 The proof can be found in App. B.1, where we show that \mathcal{X}^* , the optimal data mixture of original
189 problem 2, satisfies a mixing ratio r^* that is also the solution of reparameterized problem 3. DUET
190 aims to solve problem 3 in an iterative manner. At the outer optimization level (global), DUET
191 uses BO to exploit feedback from the evaluation task to propose a promising mixing ratio r_t at each
192 iteration t . At the inner optimization level (local), we introduce a sampling strategy that uses local
193 domain data selection to retrieve a high-quality data subset that satisfies mixing ratio r_t .
194

195 3.2 USING DATA SELECTION METHODS FOR INNER PROBLEM

196 In this section, we show how data selection methods can be used to solve the inner problem in DUET.
197 **For ease of expository and illustration, we use Influence Function (IF) as the choice of data
198 selection method to explain our method.** DUET is flexible enough to incorporate different data
199 selection choice and we analyzed different data selection methods in our experiments (Sec. 6). Our
200 inner optimization problem aims to find the best-performing data mixture that satisfies:
201

$$\mathcal{X}_r^* \triangleq \arg \min_{\mathcal{X} \in S_r} \mathcal{L}_{\text{eval}}(\theta_{\mathcal{X}}), \quad (4)$$

202 where $S_r \triangleq \{\mathcal{X} : \text{ratio}(\mathcal{X}) = r, |\mathcal{X}| = M\}$. In other words, we need to find a subset of data \mathcal{X}_r^* that
203 yields the lowest evaluation task loss $y_r^* = \mathcal{L}_{\text{eval}}(\theta_{\mathcal{X}_r^*})$ while constrained to mixing ratio r .
204

205 First, let’s consider a simple approach, based on prior works on estimating distribution extrema
206 (de Haan, 1981; Lee & Miller, 2022). We randomly sample k different data mixtures from S_r .
207 This yields k data mixture samples $\{\mathcal{X}_1, \dots, \mathcal{X}_k\}$ (each satisfying the mixing ratio r). A **uniform**
208 **random estimator** for y_r^* is obtained by evaluating the unseen task performance of an LLM trained
209 on each data mixture sample and taking the minimum: $\tilde{y}_r^* = \min_{\mathcal{X}_i} \{\mathcal{L}_{\text{eval}}(\theta_{\mathcal{X}_1}), \dots, \mathcal{L}_{\text{eval}}(\theta_{\mathcal{X}_k})\}$
210 with $\tilde{\mathcal{X}}_r^* = \arg \min_{\mathcal{X}_i} \{\mathcal{L}_{\text{eval}}(\theta_{\mathcal{X}_1}), \dots, \mathcal{L}_{\text{eval}}(\theta_{\mathcal{X}_k})\}$ as the solution estimate of inner problem 4. The
211 estimator \tilde{y}_r^* is the 1st-order statistic (Arnold et al., 2008) and a random variable. While consistent
212 (i.e., as we increase the sampling size k , we can estimate the solution of Eq. 4 more accurately),
213 uniform random estimator \tilde{y}_r^* has high variance (we provide empirical evidence in Fig. 8) because
214 from k uniformly random data mixture samples, it is unlikely we select the optimal data mixture.
215

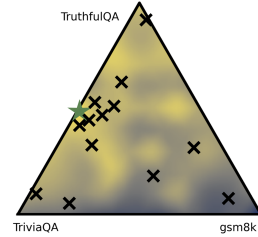


Figure 2: DUET finds the optimal data mixture iteratively and strategically.

216 **How can data selection help?** We aim to improve the quality of estimator \tilde{y}_r^* by incorporating data
 217 selection methods (Sim et al., 2022; Wang et al., 2024a) into our sampling process. Specifically, we
 218 want to increase the chance of sampling high-quality data points (conversely, reduce the chance of
 219 sampling low-quality data points) from each data domain, before using it to train an LLM. To do
 220 so, let us consider the use of influence function (Koh & Liang, 2017; Saunshi et al., 2023) (IF) as a
 221 data selection method into our estimator \tilde{y}_r^* to estimate the inner problem solution more accurately.
 222 In App. A.5, we discuss the tradeoffs between different data selection methods, such as coressets
 223 (Mirzasoleiman et al., 2020), diversity-driven measures (Wang et al., 2024b) and LESS (Xia et al.,
 224 2024) when used in DUET. Our experimental results (Fig. 6) also analyzed the performance of DUET
 225 paired with different data selection methods.

226 **IF-driven estimator.** We construct an IF-driven estimator in the following manner: *first*, for each
 227 dataset $D_i \in \mathcal{D}$ from the training domains, we fine-tune a separate, potentially smaller, LLM on
 228 that dataset. *Second*, we derive the IF score of each training data point w.r.t. the trained LLM for its
 229 respective domain (this can be computed and stored beforehand; more details in App. A.4). *Lastly*,
 230 given a mixing ratio r proposed at each iteration, we perform weighted sampling from each domain
 231 based on each data point’s IF score within the domain dataset (instead of uniform sampling as
 232 mentioned previously) until we satisfy the mixing ratio r . From hereon, we refer to this sampling
 233 process as *IF-weighted sampling*. For each data domain, there is a higher chance to sample a data
 234 point with a higher IF score. This yields a data mixture sample \mathcal{X}^{IF} . By performing IF-weighted
 235 sampling k times, we obtain k samples of IF-weighted data mixtures $\{\mathcal{X}_1^{IF}, \dots, \mathcal{X}_k^{IF}\}$, producing a
 236 new **IF-driven estimator**:

$$237 \tilde{y}_r^* = \min_{\mathcal{X}_i} \{\mathcal{L}_{\text{eval}}(\theta_{\mathcal{X}_1^{IF}}), \dots, \mathcal{L}_{\text{eval}}(\theta_{\mathcal{X}_k^{IF}})\}, \quad (5)$$

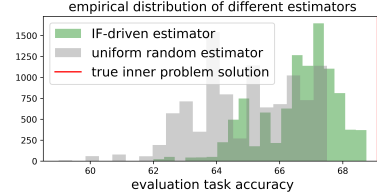
238 which estimates the solution of inner optimization problem 4. Unlike the uniform random estimator
 239 mentioned earlier, IF-driven estimator emphasizes selecting data with high IF scores, and prior works
 240 (Saunshi et al., 2023) have regarded data points with higher IF scores as of higher quality. Next, we
 241 will discuss the empirical distribution of the IF-driven estimator.

242 **Empirical distribution.** In Fig. 3, we mixed data from two
 243 training domains to train an LLM to maximize an unseen task
 244 accuracy (while Eq. 4 & 5 consider the minimization case,
 245 we can use max instead of min for the maximization case).
 246 We used a fixed mixing ratio $r = [0.5, 0.5]$. The optimal data
 247 mixture satisfying this ratio attains a task accuracy indicated
 248 by the **red line** (obtained by iterating through all possible data
 249 mixtures in a brute-force manner). Ideally, we want our esti-
 250 mator to be as close to the red line as possible. Next, we plot
 251 the empirical distribution of the **uniform random estimator**
 252 and **IF-driven estimator**. Empirically, the IF-driven estimator
 253 (**green histogram**) has a lower variance and bias than the uni-
 254 form random estimator (**gray histogram**), producing a closer estimate to the true solution (**red line**).
 255 This suggests that the IF-driven estimator \tilde{y}_r^* estimates the solution of problem 4 more accurately.

256 **Theoretical distribution.** Exactly how well does the IF-driven estimator \tilde{y}_r^* estimate the optimal
 257 unseen evaluation task loss y_r^* w.r.t. a given data ratio r ? To answer this, we theoretically analyze this
 258 estimator’s empirical distribution. Empirically (App. A.7), the negative of the sampling distribution of
 259 the unseen task accuracy (we consider the negative because we are looking to maximize the accuracy,
 260 instead of minimizing the loss) of each sample $\mathcal{L}_{\text{eval}}(\theta_{\mathcal{X}_i^{IF}})$ resembles a truncated exponential
 261 distribution. Based on this, we characterize how well the IF-driven estimator \tilde{y}_r^* estimates y_r^* :

262 **Theorem 3.2.** Let $\{\mathcal{X}_1^{IF}, \dots, \mathcal{X}_k^{IF}\}$ be k data mixture samples drawn from S_r using IF-weighted
 263 sampling. Furthermore, assume each independent sample $\mathcal{L}_{\text{eval}}(\theta_{\mathcal{X}_i^{IF}})$ follows the shifted truncated
 264 exponential distribution $y_r^* + \exp_t(\lambda, c)$, for $i = 1, 2, \dots, k$ where $\exp_t(\lambda, c)$ is a truncated exponential
 265 distribution governed by rate parameter λ and truncated at $c > 0$. Then, the IF-driven estimator
 266 \tilde{y}_r^* defined in Eq. 5 is a random variable: $y_r^* + \epsilon$, where y_r^* is the true inner problem solution of Eq. 4
 267 and ϵ is a random noise variable with probability density function (PDF):

$$268 \text{PDF}_\epsilon(u) = \frac{\lambda e^{-\lambda u}}{1 - e^{-\lambda c}} \left(\frac{e^{-\lambda u} - e^{-\lambda c}}{1 - e^{-\lambda c}} \right)^{k-1} \text{ on } u \in [0, c].$$



269 Figure 3: Empirical distribution of the uniform random and IF-driven estimator \tilde{y}_r^* . **Red line** is the true
 270 inner problem solution.

270 The proof is shown in App. B.2 and computes the probability distribution of the 1st order statistic (in
 271 which our estimator uses) of a truncated exponential distribution. Theorem 3.2 is used in DUET’s
 272 convergence analysis in Sec. 4. In App. B.4, we also provide details to help readers extend our
 273 analysis to other empirical sampling distributions. This also indicates that estimation error ϵ of the
 274 IF-driven estimator reduces to 0 as the sampling size k increases asymptotically. Surprisingly, our
 275 experiments (Sec. 6) show that using $k = 1$ is enough to select good data mixtures, underscoring
 276 the effectiveness of using data selection as opposed to random sampling. We also found that given
 277 sufficient budget, using varying k gives us granular control of DUET’s performance (Sec. 6.3).

279 3.3 USING BAYESIAN OPTIMIZATION FOR OUTER PROBLEM

280 With the IF-driven estimator introduced to estimate the inner optimization problem solution (or any
 281 estimator using a desired data selection method of choice), we shift our focus to solving the outer
 282 optimization problem of problem 3, which aims to find the optimal data mixing ratio r^* for the unseen
 283 evaluation task. Since the solution of the inner problem $y_r^* = \min_{\mathcal{X} \in S_r} \mathcal{L}_{\text{eval}}(\theta_{\mathcal{X}})$ depends only on
 284 the mixing ratio r , we can define a function $f(r) \triangleq y_r^* = \min_{\mathcal{X} \in S_r} \mathcal{L}_{\text{eval}}(\theta_{\mathcal{X}})$, where for a given
 285 mixing ratio r , we use the IF-driven estimator to estimate a solution for the inner problem, producing
 286 $f(r)$. As such, the outer optimization problem of problem 3 can be rewritten into $\min_r f(r)$ where
 287 $r \in \mathbb{R}^n$ is a probability simplex representing the mixing ratio over the n training domains. DUET
 288 uses BO constrained to $\|r\|_1 = 1$ (Sec. 2.1) to find the optimal mixing ratio r^* for the outer problem.

289 BO is suitable for solving this problem for a few reasons. First, evaluating f requires us to use
 290 the IF-driven estimator to estimate the inner optimization problem solution and thus f is a black-
 291 box function with no closed, mathematical form; BO is a principled and popular framework to
 292 optimize such black-box functions (Garnett, 2023; Pyzer-Knapp, 2018). Second, we are estimating
 293 the inner problem solution (Theorem. 3.2) using data selection. This implies we can only obtain
 294 *noisy observations* $f(r) + \epsilon$, where ϵ is a random noise variable with the same distribution as that in
 295 Theorem 3.2; fortunately, BO handles noisy function observations gracefully (Srinivas et al., 2010;
 296 Chowdhury & Gopalan, 2017) during the optimization process, allowing us to find the optimal mixing
 297 ratio eventually (theoretical results shown in Sec. 4).

299 3.4 INTERLEAVING THE IF-DRIVEN ESTIMATOR AND BO

300 DUET uses BO at the outer level and IF-driven estimator at the inner level to iteratively optimize the
 301 data mixture, solving problem 3. We formally describe DUET in Algorithm 1.

304 **Algorithm 1** DUET: Optimizing training Data Mixtures for an Unseen Evaluation Task

- 305 1: **Input:** n training datasets from n domains $\{D_1, \dots, D_n\}$. Computed IF scores of each data
 306 point (App. A.4) w.r.t. its domain dataset and locally trained model. Initial observation of data
 307 mixing ratio and evaluation task performance: $\mathcal{D}_0 \triangleq \{(r_0, \tilde{y}_0)\}$, SE kernel κ , sampling size k ,
 308 parameter β_t for acquisition step and total number of BO iterations T .
- 309 2: **for** $t = 1, \dots, T$ **do**
- 310 3: $r_t = \arg \min_r \mu_t(r) - \beta_t \sigma_t(r)$ (BO acquisition step)
- 311 4: IF-weighted sampling to obtain k samples of data mixtures $\{\mathcal{X}_1^{IF}, \dots, \mathcal{X}_k^{IF}\}$ (Sec. 3.2).
- 312 5: **IF-driven estimator** at iteration t :
 313 $\tilde{y}_{r_t}^* = \min_{\mathcal{X}_i} \{\mathcal{L}_{\text{eval}}(\theta_{\mathcal{X}_1^{IF}}), \dots, \mathcal{L}_{\text{eval}}(\theta_{\mathcal{X}_k^{IF}})\}$.
- 314 6: Keep track of best performing data mixture $\mathcal{X}_t^* = \arg \min_{\mathcal{X}_i} \{\mathcal{L}_{\text{eval}}(\theta_{\mathcal{X}_1^{IF}}), \dots, \mathcal{L}_{\text{eval}}(\theta_{\mathcal{X}_k^{IF}})\}$.
- 315 7: $\mathcal{D}_t = \mathcal{D}_{t-1} \cup \{(r_t, \tilde{y}_{r_t}^*)\}$
- 316 8: Update the GP posterior and κ with updated observations \mathcal{D}_{t+1} (Sec. 2.1).
- 317 9: **end for**
- 318 10: $\mathcal{X}^* = \arg \min_{\mathcal{X}_i^* \in \{\mathcal{X}_1^*, \dots, \mathcal{X}_T^*\}} \mathcal{L}_{\text{eval}}(\theta_{\mathcal{X}_i^*})$

321 At iteration t , DUET uses the LCB acquisition function (Srinivas et al., 2010) on the GP posterior to
 322 propose a candidate mixing ratio r_t for our data domains (Line 3). Using the proposed mixing ratio
 323 r_t , we use IF scores of each data point to compute the IF-driven estimator $\tilde{y}_{r_t}^*$ and fine-tune an LLM
 with the selected data points and observe the feedback from the downstream unseen task based on the

324 fine-tuned LLM. We keep track of the best performing data mixture sample \mathcal{X}_t^* at every iteration t
 325 (Line 4, 5 and 6). Next, we include $(r_{t+1}, \widetilde{y}_{r_t}^*)$ into our historical observations \mathcal{D}_{t+1} (Line 7) and
 326 update our GP posterior (Line 8). After which, we repeat the entire feedback process to select the
 327 next LLM fine-tuning data mixture, until the budget of T BO iterations is exhausted. In the end, we
 328 recover the best performing data mixture \mathcal{X}^* for the unseen evaluation task (Line 10).
 329

330 4 THEORETICAL ANALYSIS

332 4.1 CONVERGENCE ANALYSIS OF DUET USING CUMULATIVE REGRET

334 We analyze the convergence rate of DUET using the growth of *attained cumulative regret* (Chen et al.,
 335 2024b) $\tilde{R}_T = \sum_{t=1}^T |\widetilde{y}_{r_t}^* - f(r_t)| = \sum_{t=1}^T |f(r^*) + \epsilon_t - f(r_t)|$ for T BO iterations. The attained
 336 cumulative regret consists of two terms, where $|f(r^*) - f(r_t)|$ indicates the quality of mixing ratio r_t
 337 proposed at each iteration while ϵ_t indicates how well we can estimate the inner problem solution at
 338 every iteration. By analyzing the attained *average* regret \tilde{R}_T/T with $T \rightarrow \infty$, the following Theorem
 339 helps us understand how close our algorithm converges (Berkenkamp et al., 2019).

340 **Theorem 4.1.** *Let f be the outer problem objective defined in Sec. 3.3 with bounded RKHS norm:
 341 $\|f\|_\kappa = \sqrt{\langle f, f \rangle_\kappa}$. Also, let our IF-driven estimator for the inner problem solution be governed by the
 342 error distribution introduced in Theorem 3.2 with constant c and $\lambda = 1$. Let $A_{c,k} = \frac{c^2(1-e^{-c}-\frac{c}{2})^{k-1}}{(1-e^{-c})^k}$,
 343 where k is a fixed predecided sampling size. Then, running DUET over f using the LCB acquisition
 344 function found in (Chowdhury & Gopalan, 2017) at each BO iteration $t = 1, \dots, T$ yields the
 345 following **attained average regret** (Chen et al., 2024b) upper bound with probability at least $1 - \delta$:*

$$347 \lim_{T \rightarrow \infty} \frac{\tilde{R}_T}{T} \leq \frac{6(\sqrt[4]{\delta} + \sqrt{k})}{\sqrt[4]{\delta}k} + 2A_{c,k} + \frac{\sqrt{2A_{c,k}}}{\sqrt[4]{\delta}}.$$

350 The proof is provided in App. B.3 and bounds $|f(r^*) - f(r_t)|$ and ϵ_t independently using BO regret
 351 analysis (Chen et al., 2024b; Chowdhury & Gopalan, 2017) and the error distribution defined in
 352 Theorem 3.2. Our Theorem's average regret indicates how close our algorithm converges to the
 353 optimal evaluation task loss with increasing BO iteration T and different choices of sampling size
 354 k . Notice that because c characterizes the error of our estimator in Theorem 3.2, a larger c would
 355 decrease $A_{c,k}$ and our average regret. In addition, a larger sampling size k reduces the estimation
 356 error of the inner problem (Theorem. 3.2), decreasing $A_{c,k}$ and reducing our regret bound, although
 357 our experiments (Sec. 6.2) show that setting $k = 1$ is sufficient to achieve good performance.

358 5 PRACTICAL CONSIDERATIONS

361 We are free to use any data selection methods in DUET's inner loop. We specifically highlighted IF as
 362 a data selection method because in our experiments, IF worked slightly better when paired with BO
 363 (see Fig. 6 for detailed ablation) as compared to other selection methods. It also has some interpretable
 364 advantages (Sec. A.6). Even though computing IF scores could be budget-intensive, practical tricks,
 365 such as parallel computation, Hessian approximation (Agarwal et al., 2017), pre-computation, or a
 366 smaller surrogate model can speed up computation.

367 If scaling to large-scale datasets is too compute-intensive, one could also use cheaper data selection
 368 methods in DUET, such as LESS (Xia et al., 2024) or TracIn (Pruthi et al., 2020) with some
 369 performance-tradeoff. In the extreme case, one can even resort to the uniform random estimator
 370 introduced in Sec. 3.2, which does not perform any data selection. We experimented with DUET
 371 paired with different data selection methods in Sec. 6.3 and discussed their actual compute-time
 372 in App. C.1. In addition, DUET's iterative optimization process is a feature: subjecting LLMs to
 373 multiple rounds of training in a feedback loop is a natural part of its deployment life-cycle.

374 6 EXPERIMENTS AND DISCUSSION

375 We conduct extensive experiments to showcase the effectiveness of DUET compared to other baselines.
 376 We optimize data mixtures with different methods based on multiple rounds of evaluation task

378 performance feedback. Then, we fine-tune an LLM with the optimized data mixture. Lastly, we
 379 deploy the LLM on the evaluation task to evaluate how well the model has performed. We provide
 380 more details of our experimental setup and our algorithm computational cost in App. C.1.
 381

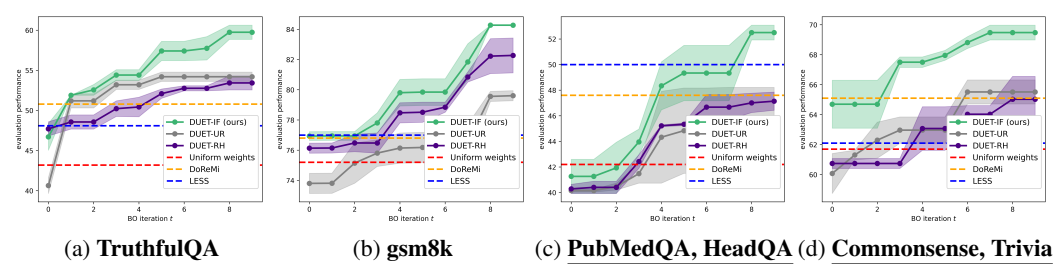
382 6.1 EXPERIMENTAL SETUP

384 Our experiments are carried out by performing PEFT (Hu et al., 2021) of `Llama-3-8b-Instruct`
 385 (Touvron et al., 2023) across different LLM knowledge domains. We also ran our experiments with
 386 `Qwen2.5-7B-Instruct` (Qwen et al., 2025) and present the results in App. C.3. Our findings
 387 were similar even for different LLMs. The training data domains for LLM evaluation consists of 9
 388 topics: **Wikitext** (Merity et al., 2016), **gsm8k** (Cobbe et al., 2021), **PubmedQA** (Jin et al., 2019),
 389 **HeadQA** (Vilares & Gómez-Rodríguez, 2019), **SciQ** (Welbl et al., 2017), **TriviaQA** (Joshi et al.,
 390 2017), **TruthfulQA** (Lin et al., 2022), **Hellaswag** (Zellers et al., 2019), and **CommonsenseQA**
 391 (Talmor et al., 2019). We also varied the difficulty of the unseen task by making them out-of-domain
 392 (see captions of Fig. 4). Our LLM performance might have slight differences from existing papers,
 393 most likely due to evaluation setup differences, which we elaborate in App. C.1.
 394

395 We ran several baselines: **DoReMi** (Xie et al., 2023a) is a data-mixing approach that optimizes the
 396 data mixture in a distributionally robust manner. **LESS** (Xia et al., 2024) is a data-selection method
 397 based on data gradient similarities. The **Uniform weights** baseline uses a data mixture of uniform
 398 ratio across different domains. We ran our baselines for the same number of iterations at DUET
 399 and take the best performing result to ensure similar compute comparison. We also used DUET
 400 with a few different data selection methods: **DUET-IF** uses our IF-driven estimator (Eq. 5) to select
 401 data mixtures at each BO iteration; **DUET-UR**, introduced in Sec. 3.2, uses the uniform random
 402 estimator and randomly selects data mixtures that satisfy the proposed mixing ratio; **DUET-RH**
 403 (**Remove Harmful**) removes 20% of data points with the lowest IF scores from each data domain,
 404 before performing sampling. **DUET-LESS** (Xia et al., 2024) and **DUET-logdet** (Wang et al., 2024b),
 405 which incorporate different data selection methods into DUET, were also used in our ablation studies
 406 (Fig. 6). We used a sampling size of $k = 1$ and BO iterations $T = 10$. We also constrained the total
 407 number of selected data points to $M = 10000$ with a temperature of 0.75 in our LLMs. This makes
 408 the "feedback" (performance) of all valuation tasks *noisy*, similar to real-world tasks.
 409

410 We also compared DUET with other baselines, such as **Aioli** (Chen et al., 2024a), **Multi-fidelity**
 411 **BO** (Yen et al., 2025), **online data-mixing** (Albalak et al., 2023a), alongside naive approaches: e.g.,
 412 using more training tokens, random search or only data selection. Due to space constraints, we show
 413 these results in Table. 2. In general, DUET still finds better data mixtures than these baselines.
 414

415 6.2 MAIN RESULT



417 Figure 4: Results on unseen LLM evaluation task domains over 10 iterations (higher is better)
 418 for `Llama-3-8b-Instruct`. Experiments were repeated with `Qwen2.5-7b-Instruct` in
 419 App. C.3. The caption shows the evaluation task. **Underlined evaluation tasks are harder** because
 420 the evaluation task domains are removed from the training data (i.e., out-of-domain). Results for
 421 more baselines are presented in Table. 1.
 422

423 **DUET finds more optimal data mixtures.** Our result (Fig. 4) shows that DUET finds better data
 424 mixtures within a few iterations of feedback loops. The first column in Fig. 4 consists of a relatively
 425 easier task where the evaluation domain is part of the training task domains. In this case, DUET
 426 (**green plot**) uses feedback from the evaluation task to find the optimal data mixture with more weights
 427

on the relevant training data domain, TruthfulQA. On the other hand, we observe the weakness of conventional methods which cannot exploit coarse feedback: DoReMi (orange dotted line) and LESS (orange dotted line) both cannot specifically adapt to the evaluation task and hence do not perform as well. In the 2nd, 3rd and 4th columns, we increased the difficulty of our evaluation task by removing the evaluation task domain from our training domains (**the evaluation task is now out-of-domain**). Surprisingly, DUET still can use feedback from the unseen task to automatically optimize the data mixture, achieving better LLM performance than other baselines. This suggests data from another training domain is still useful for the out-of-domain evaluation task (e.g., **Wikitext** data can still be helpful for mathematical questions in **gsm8k**). Hence, DUET is effective in both in-domain and out-of-domain tasks. In App. C.4, we qualitatively discuss the optimal mixing ratios found by DUET.

6.3 ABLATION EXPERIMENTS

While we have shown that DUET outperforms existing baselines, we also ran several ablations (using Fig. 4d setting) to tease apart several components in DUET.

Ablation of different components in DUET. Fig. 5 shows the importance of both BO and data selection techniques in DUET. If we used a uniform data mixture to train an LLM, we can only achieve a baseline performance given by the red dotted line. With just BO, DUET automatically reconfigures the mixing ratio and attains performance gain (**A**). Next, by incorporating data selection methods, such as using IF in DUET-IF, we attain further performance gains (**B**) indicated by the green plot. Different data selection methods used in DUET also improves the LLM’s performance to a different extent (**C**). Therefore, this affirms the importance of interleaving data selection and BO.

Ablation of using different data selection methods in DUET. How do different data selection methods fare when used in DUET’s inner loop? In Fig. 6, we found that IF outperforms other data selection methods (LESS, RH, log-det (Wang et al., 2024b)) when used in DUET’s inner loop. This suggests that IF retrieves higher-quality (or remove lower-quality) data points at each iteration better than other methods. This aligns with our discussion in App. A.5 where we explained how IF, being able to remove low-quality data, yields better training data mixture in our unseen task setting. All in all, we are free to use different data selection techniques (each with different computational cost, performance) in DUET’s inner loop.

Ablation of varying sampling size k . Lastly, we also found that increasing sampling size k in DUET’s inner loop (Fig. 7) helps DUET find more optimal training data mixtures. This aligns with our theoretical findings from Theorem 4.1, which shows that larger k improves DUET’s convergence. In practical settings, if budget permits, LLM owners can fine-tune multiple copies of LLMs (i.e., increase k) to improve DUET’s performance. However, our results in Fig. 4 showed that even with $k = 1$, DUET outperforms other baselines.

7 CONCLUSION AND LIMITATIONS

Our paper proposes DUET, a novel algorithm that exploits multiple rounds of coarse, noisy feedback from a downstream unseen evaluation task to automatically optimize training data mixture for LLMs. Our approach offers an effective solution to address the unseen task setting, where fine-grained data information is unavailable (and conventional approaches fail). It is also quite flexible, allowing us to choose amongst different data selection methods in its inner loop. We provide theoretical guarantees of DUET and empirically show that it optimizes data mixtures in a variety of LLM evaluation tasks better than other baselines. One limitation is that our paper focused on LLM fine-tuning, but broadly speaking, we believe that DUET can be adapted to and would work equally well for pre-training. This leaves room for fruitful future research.

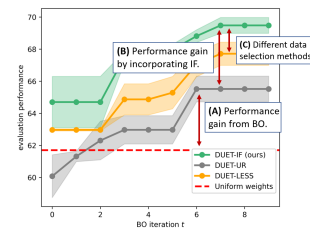


Figure 5: Ablation of different components of DUET.

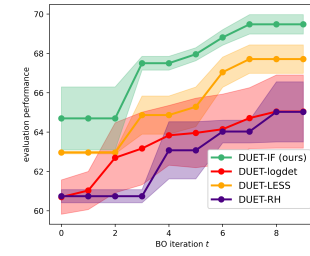


Figure 6: Ablation of using different data selection methods in DUET.

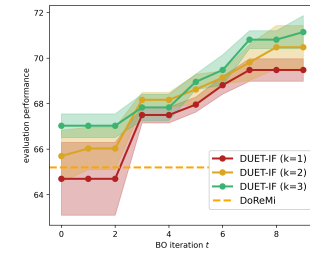


Figure 7: Ablation of sampling size k in DUET.

486 8 ETHICS STATEMENT
487488 Our work strives to improve the performance of LLMs for the greater good. We do not foresee any
489 ethical concerns related to our work. From our theoretical findings and experiments, our work can
490 also handle noisy real-world feedbacks robustly.
491492 REFERENCES
493494 Naman Agarwal, Brian Bullins, and Elad Hazan. Second-order stochastic optimization for machine
495 learning in linear time. *arXiv:1602.03943*, 2017.496 Alon Albalak, Liangming Pan, Colin Raffel, and William Yang Wang. Efficient online data mixing
497 for language model pre-training. *arXiv:2312.02406*, 2023a.
498499 Alon Albalak, Liangming Pan, Colin Raffel, and William Yang Wang. Efficient online data mixing
500 for language model pre-training. *arXiv:2312.02406*, 2023b.
501502 Alon Albalak, Yanai Elazar, Sang Michael Xie, Shayne Longpre, Nathan Lambert, Xinyi Wang,
503 Niklas Muennighoff, Bairu Hou, Liangming Pan, Haewon Jeong, Colin Raffel, Shiyu Chang,
504 Tatsunori Hashimoto, and William Yang Wang. A survey on data selection for language models.
505 *arXiv:2402.16827*, 2024.
506506 Julyan Arbel, Olivier Marchal, and Hien D. Nguyen. On strict sub-gaussianity, optimal proxy variance
507 and symmetry for bounded random variables, 2019.
508509 Barry C Arnold, Narayanaswamy Balakrishnan, and Haikady Navada Nagaraja. *A first course in*
510 *order statistics*. SIAM, 2008.
511511 Felix Berkenkamp, Angela P. Schoellig, and Andreas Krause. No-regret bayesian optimization with
512 unknown hyperparameters. In *Proc. ICML*, 2019.
513514 Mayee F. Chen, Michael Y. Hu, Nicholas Lourie, Kyunghyun Cho, and Christopher Ré. Aioli: A
515 unified optimization framework for language model data mixing. *arXiv:2411.05735*, 2024a.
516517 Zhihang Chen, Chuan-Sheng Foo, and Bryan Kian Hsiang Low. Towards AutoAI: Optimizing a
518 machine learning system with black-box and differentiable components. In *Proc. ICML*, 2024b.
519520 Sayak Ray Chowdhury and Aditya Gopalan. On kernelized multi-armed bandits. In *Proc. ICML*,
521 2017.
522523 Karl Cobbe, Vineet Kosaraju, Mohammad Bavarian, Mark Chen, Heewoo Jun, Lukasz Kaiser,
524 Matthias Plappert, Jerry Tworek, Jacob Hilton, Reiichiro Nakano, Christopher Hesse, and John
525 Schulman. Training verifiers to solve math word problems. *arXiv:2110.14168*, 2021.
526527 Laurens de Haan. Estimation of the minimum of a function using order statistics. *Journal of the*
528 *American Statistical Association*, 76(374):467–469, 1981.
529530 Simin Fan, Matteo Pagliardini, and Martin Jaggi. Doge: Domain reweighting with generalization
531 estimation. *arXiv:2310.15393*, 2024.
532533 Peter I Frazier. A tutorial on Bayesian optimization. *arXiv:1807.02811*, 2018.
534535 Yaroslav Ganin and Victor Lempitsky. Unsupervised domain adaptation by backpropagation. In *Proc.*
536 *ICML*, 2015.
537538 Leo Gao, Jonathan Tow, Baber Abbasi, Stella Biderman, Sid Black, Anthony DiPofi, Charles Foster,
539 Laurence Golding, Jeffrey Hsu, Alain Le Noac'h, Haonan Li, Kyle McDonell, Niklas Muennighoff,
540 Chris Ociepa, Jason Phang, Laria Reynolds, Hailey Schoelkopf, Aviya Skowron, Lintang Sutawika,
541 Eric Tang, Anish Thite, Ben Wang, Kevin Wang, and Andy Zou. A framework for few-shot
542 language model evaluation, 07 2024. URL <https://zenodo.org/records/12608602>.
543544 Jacob Gardner, Matt Kusner, Xu Zhixiang, Kilian Weinberger, and John Cunningham. Bayesian
545 optimization with inequality constraints. In *Proc. ICML*, 2014.
546

540 Roman Garnett. *Bayesian Optimization*. Cambridge Univ. Press, 2023.
 541

542 Ce Ge, Zhijian Ma, Daoyuan Chen, Yaliang Li, and Bolin Ding. Bimix: A bivariate data mixing law
 543 for language model pretraining. *arXiv:2405.14908*, 2025.

544

545 Stewart Greenhill, Santu Rana, Sunil Gupta, Pratibha Vellanki, and Svetha Venkatesh. Bayesian
 546 optimization for adaptive experimental design: A review. *IEEE Access*, 8:13937–13948, 2020. doi:
 547 10.1109/ACCESS.2020.2966228.

548

549 Ziyao Guo, Kai Wang, George Cazenavette, Hui Li, Kaipeng Zhang, and Yang You. Towards lossless
 550 dataset distillation via difficulty-aligned trajectory matching. *arXiv:2310.05773*, 2024.

551

552 Jordan Hoffmann, Sebastian Borgeaud, Arthur Mensch, Elena Buchatskaya, Trevor Cai, Eliza Rutherford,
 553 Diego de las Casas, Lisa Anne Hendricks, Johannes Welbl, Aidan Clark, Tom Hennigan,
 554 Eric Noland, Katherine Millican, George van den Driessche, Bogdan Damoc, Aurelia Guy, Simon
 555 Osindero, Karen Simonyan, Erich Elsen, Oriol Vinyals, Jack William Rae, and Laurent Sifre. An
 556 empirical analysis of compute-optimal large language model training. In *Proc. NeurIPS*, 2022.

557

558 Edward J. Hu, Yelong Shen, Phillip Wallis, Zeyuan Allen-Zhu, Yuanzhi Li, Shean Wang, Lu Wang,
 559 and Weizhu Chen. Lora: Low-rank adaptation of large language models. *arXiv:2106.09685*, 2021.

560

561 Neil Jethani, Mukund Sudarshan, Ian Covert, Su-In Lee, and Rajesh Ranganath. Fastshap: Real-time
 562 shapley value estimation. *arXiv:2107.07436*, 2022.

563

564 Qiao Jin, Bhuwan Dhingra, Zhengping Liu, William W. Cohen, and Xinghua Lu. Pubmedqa: A
 565 dataset for biomedical research question answering. *arXiv:1909.06146*, 2019.

566

567 Mandar Joshi, Eunsol Choi, Daniel S. Weld, and Luke Zettlemoyer. Triviaqa: A large scale distantly
 568 supervised challenge dataset for reading comprehension. *arXiv:1705.03551*, 2017.

569

570 Diederik P. Kingma and Jimmy Ba. Adam: A method for stochastic optimization, 2017.

571

572 Pang Wei Koh and Percy Liang. Understanding black-box predictions via influence functions. In
 573 *Proc. ICML*, 2017.

574

575 Anthony Lee and Steven J Miller. Generalizing the german tank problem. *arXiv:2210.15339*, 2022.

576

577 Tianshi Li, Sauvik Das, Hao-Ping Lee, Dakuo Wang, Bingsheng Yao, and Zhiping Zhang. Human-
 578 centered privacy research in the age of large language models. *arXiv:2402.01994*, 2024.

579

580 Stephanie Lin, Jacob Hilton, and Owain Evans. Truthfulqa: Measuring how models mimic human
 581 falsehoods. *arXiv:2109.07958*, 2022.

582

583 Mingsheng Long, Han Zhu, Jianmin Wang, and Michael I. Jordan. Deep transfer learning with joint
 584 adaptation networks. In *Proc. ICML*, 2017.

585

586 Stephen Merity, Caiming Xiong, James Bradbury, and Richard Socher. Pointer sentinel mixture
 587 models. *arXiv:1609.07843*, 2016.

588

589 Baharan Mirzasoleiman, Jeff Bilmes, and Jure Leskovec. Coresets for data-efficient training of
 590 machine learning models. *arXiv:1906.01827*, 2020.

591

592 Krikamol Muandet, David Balduzzi, and Bernhard Schölkopf. Domain generalization via invariant
 593 feature representation. *arXiv:1301.2115*, 2013.

594

595 Garima Pruthi, Frederick Liu, Mukund Sundararajan, and Satyen Kale. Estimating training data
 596 influence by tracing gradient descent. *arXiv:2002.08484*, 2020.

597

598 Edward O Pyzer-Knapp. Bayesian optimization for accelerated drug discovery. *IBM Journal of
 599 Research and Development*, 62(6):2–1, 2018.

594 Qwen, :, An Yang, Baosong Yang, Beichen Zhang, Binyuan Hui, Bo Zheng, Bowen Yu, Chengyuan
 595 Li, Dayiheng Liu, Fei Huang, Haoran Wei, Huan Lin, Jian Yang, Jianhong Tu, Jianwei Zhang,
 596 Jianxin Yang, Jiaxi Yang, Jingren Zhou, Junyang Lin, Kai Dang, Keming Lu, Keqin Bao, Kexin
 597 Yang, Le Yu, Mei Li, Mingfeng Xue, Pei Zhang, Qin Zhu, Rui Men, Runji Lin, Tianhao Li,
 598 Tianyi Tang, Tingyu Xia, Xingzhang Ren, Xuancheng Ren, Yang Fan, Yang Su, Yichang Zhang,
 599 Yu Wan, Yuqiong Liu, Zeyu Cui, Zhenru Zhang, and Zihan Qiu. Qwen2.5 technical report.
 600 *arXiv:2412.15115*, 2025.

601 Nikunj Saunshi, Arushi Gupta, Mark Braverman, and Sanjeev Arora. Understanding influence
 602 functions and datamodels via harmonic analysis. In *Proc. ICLR*, 2023.

603 604 Seungjae Shin, HeeSun Bae, Byeonghu Na, Yoon-Yeong Kim, and Il chul Moon. Unknown domain
 605 inconsistency minimization for domain generalization. In *Proc. ICLR*, 2024.

606 607 Rachael Hwee Ling Sim, Xinyi Xu, and Bryan Kian Hsiang Low. Data valuation in machine learning:
 608 "ingredients", strategies, and open challenges. In *Proc. IJCAI*, 2022.

609 610 Jasper Snoek, Hugo Larochelle, and Ryan P Adams. Practical bayesian optimization of machine
 611 learning algorithms. In *Proc. NeurIPS*, 2012.

612 613 Niranjan Srinivas, Andreas Krause, Sham Kakade, and Matthias Seeger. Gaussian process optimiza-
 614 tion in the bandit setting: No regret and experimental design. In *Proc. ICML*, 2010.

615 616 Alon Talmor, Jonathan Herzig, Nicholas Lourie, and Jonathan Berant. Commonsenseqa: A question
 617 answering challenge targeting commonsense knowledge. *arXiv:1811.00937*, 2019.

618 619 Sebastian Shenghong Tay, Chuan-Sheng Foo, Daisuke Urano, Richalynn Leong, and Bryan
 620 Kian Hsiang Low. Bayesian optimization with cost-varying variable subsets. In *Proc. NeurIPS*,
 621 2023.

622 Daniel Ting and Eric Brochu. Optimal sub-sampling with influence functions. *arXiv:1709.01716*,
 2017.

623 624 Kushal Tirumala, Aram H. Markosyan, Luke Zettlemoyer, and Armen Aghajanyan. Memorization
 625 without overfitting: Analyzing the training dynamics of large language models. *arXiv:2205.10770*,
 2022.

626 627 Hugo Touvron, Thibaut Lavril, Gautier Izacard, Xavier Martinet, Marie-Anne Lachaux, Timothée
 628 Lacroix, Baptiste Rozière, Naman Goyal, Eric Hambro, Faisal Azhar, Aurelien Rodriguez, Armand
 629 Joulin, Edouard Grave, and Guillaume Lample. Llama: Open and efficient foundation language
 630 models. *arXiv:2302.13971*, 2023.

631 632 David Vilares and Carlos Gómez-Rodríguez. HEAD-QA: A healthcare dataset for complex reasoning.
 633 In *Proc. ACL*, 2019.

634 635 Jindong Wang, Cuiling Lan, Chang Liu, Yidong Ouyang, Tao Qin, Wang Lu, Yiqiang Chen, Wenjun
 636 Zeng, and Philip S. Yu. Generalizing to unseen domains: A survey on domain generalization.
 637 *arXiv:2103.03097*, 2022.

638 639 Jingtang Wang, Xiaoqiang Lin, Rui Qiao, Chuan-Sheng Foo, and Bryan Kian Hsiang Low. Helpful or
 640 harmful data? fine-tuning-free shapley attribution for explaining language model predictions. In
 641 *Proc. ICML*, 2024a.

642 643 Peiqi Wang, Yikang Shen, Zhen Guo, Matthew Stallone, Yoon Kim, Polina Golland, and
 644 Rameswar Panda. Diversity measurement and subset selection for instruction tuning datasets.
 645 *arXiv:2402.02318*, 2024b.

646 Johannes Welbl, Nelson F. Liu, and Matt Gardner. Crowdsourcing multiple choice science questions.
 647 In *Workshop on Noisy User-generated Text*, 2017.

648 Christopher KI Williams and Carl Edward Rasmussen. *Gaussian processes for machine learning*,
 649 volume 2. MIT press Cambridge, MA, 2006.

648 Mengzhou Xia, Sadhika Malladi, Suchin Gururangan, Sanjeev Arora, and Danqi Chen. Less:
 649 Selecting influential data for targeted instruction tuning. *arXiv:2402.04333*, 2024.
 650

651 Sang Michael Xie, Hieu Pham, Xuanyi Dong, Nan Du, Hanxiao Liu, Yifeng Lu, Percy Liang, Quoc V
 652 Le, Tengyu Ma, and Adams Wei Yu. Doremi: Optimizing data mixtures speeds up language model
 653 pretraining. In *Proc. NeurIPS*, 2023a.

654 Sang Michael Xie, Shibani Santurkar, Tengyu Ma, and Percy S Liang. Data selection for language
 655 models via importance resampling. In *Proc. NeurIPS*. Curran Associates, Inc., 2023b.
 656

657 Wanyun Xie, Francesco Tonin, and Volkan Cevher. Chameleon: A flexible data-mixing framework
 658 for language model pretraining and finetuning. *arXiv:2505.24844*, 2025.

659

660 Thomson Yen, Andrew Wei Tung Siah, Haozhe Chen, Tianyi Peng, Daniel Guetta, and Hongseok
 661 Namkoong. Data mixture optimization: A multi-fidelity multi-scale bayesian framework, 2025.
 662 URL <https://arxiv.org/abs/2503.21023>.

663 Rowan Zellers, Ari Holtzman, Yonatan Bisk, Ali Farhadi, and Yejin Choi. Hellaswag: Can a machine
 664 really finish your sentence? *arXiv:1905.07830*, 2019.

665

666 Bo Zhang, Xiaoming Zhang, Yun Liu, Lei Cheng, and Zhoujun Li. Matching distributions between
 667 model and data: Cross-domain knowledge distillation for unsupervised domain adaptation. In
 668 *Proc. ACL*, 2021.

669

670 Wenyu Zhang, Li Shen, Wanyue Zhang, and Chuan-Sheng Foo. Few-shot adaptation of pre-trained
 671 networks for domain shift. *arXiv:2205.15234*, 2022.

672

673 Xiaoyu Zhang, Juan Zhai, Shiqing Ma, Chao Shen, Tianlin Li, Weipeng Jiang, and Yang Liu.
 674 Speculative coresets selection for task-specific fine-tuning. *arXiv:2410.01296*, 2024.

675

676 A SUPPLEMENTARY MATERIAL

678 A.1 REAL-WORLD EXAMPLES OF OUR PROBLEM SETTING

679 In our problem setting, (a) there is no direct access to the data (e.g., its domain, distribution, or labels)
 680 involved in the unseen evaluation task but (b) multiple rounds of coarse feedback (details covered in
 681 Sec. 2.2) can be gathered from the task using a trained LLM. Here, we provide several real-world
 682 examples in which such a setting occurs.

683

684 **End-to-end encrypted conversations between LLM and users.** This setting is specific to the
 685 conversational setting between a trained LLM and human users. LLM owners are interested in fine-
 686 tuning an LLM to converse well with some human-user demographics but due to real-world privacy
 687 concerns (Li et al., 2024), conversations between a deployed LLM and users are end-to-end encrypted
 688 during test-time (openai.com/enterprise-privacy). So, an LLM owner does not have
 689 any knowledge of the conversation domain or the (unlabeled or labeled) data seen during test-time.
 690 Instead, they only receive a feedback on how well the LLM has performed in the conversation (e.g.,
 691 ratings from the human user, how long each user stays on the applicaton). The LLM owner can
 692 collect multiple rounds of feedback over a period of time. Hence, they can exploit this feedback to
 693 iteratively refine the training data mixture. Many chat-driven applications (e.g., whatsapp, telegram)
 nowadays use end-to-end encrypted chats, so our problem setting is relevant here.

694

695 **Model marketplace.** In addition, there are other scenarios in which a model owner needs to
 696 improve an ML model without having access to the data involved in the unseen evaluation task. For
 697 instance, an ML model owner might rent or sell an ML model in a model marketplace (e.g., <https://aws.amazon.com/marketplace/solutions/machine-learning>). However, the
 698 consumer might give feedback (e.g., how often the model makes mistakes) to the ML model owner
 699 in hope that the ML model owner can improve the model’s performance on its own evaluation task.
 700 Furthermore, the data used by the consumer in its evaluation task are considered sensitive data, so the
 701 ML model owner does not know any data involved in the unseen evaluation task. Hence, the ML
 owner can only rely on feedback from the consumer to improve the training data mixture.

702 A.2 MORE RELATED WORKS ON DATA MIXING AND SELECTION
703

704 Recently, a large class of data selection methods utilizing coresets (Zhang et al., 2024), diversity
705 measures (Wang et al., 2024b), gradient information (Xia et al., 2024) or influence function (Koh &
706 Liang, 2017) has been introduced to retrieve a smaller subset of data from an existing dataset. These
707 data selection methods have become popular because they reduce training dataset size (which is an
708 attractive feature when training LLMs) and prior work (Xia et al., 2024) showed that training a model
709 with strategically selected data points allows it to perform better. In addition, data mixing works
710 (Xie et al., 2023a; Ge et al., 2025; Albalak et al., 2023b) have studied how to reweigh different data
711 domains to produce optimal data mixtures, using distributionally robust optimization or entropy-based
712 signals. However, these works, when used in isolation, **do not work well in our setting because they**
713 **do not exploit feedback from an unseen evaluation task.** For example, even if we can retrieve a
714 high-quality data subset from the training data domain, this domain might not even be relevant to the
715 unseen evaluation task. Hence, data mixing and selection methods on their own **are not applicable**
716 **to our setting** because they have no way to discern how relevant the training data domain is to the
717 unseen task. Instead, our paper’s algorithm interleaves BO and data selection method together to
718 exploit feedback from the unseen evaluation task to optimize our training data mixture. Indeed, our
719 experimental results in Sec. 6.2 show that DUET performs better than other data mixing and selection
720 works.

721 A.3 EXTENSIONS AND DISCUSSION OF DUET IN OTHER SPECIAL SETTINGS
722

723 Here, we discuss some extensions of DUET to other settings that fall beyond the scope of our paper.
724 However, we find them insightful and useful when implementing DUET in practice.

725 **Should we re-fine-tune/re-train the LLM from scratch each time in DUET or continue training**
726 **the model from the previous iteration?** Our problem formulation in Sec. 2.2 and theoretical findings
727 (Sec. 4) assumes DUET re-train the LLM from the same initial checkpoint at every iteration. This is
728 necessary to ensure our surrogate function landscape in GP remains consistent throughout the BO
729 process, allowing DUET to converge. From a practical perspective, we speculate that DUET will be
730 less effective if we continue training an LLM from the previous iteration. This is because training
731 data mixtures from earlier iterations might not be useful for the unseen evaluation task and the model
732 might memorize (Tirumala et al., 2022) irrelevant information that are difficult to be overwritten in
733 later BO iterations.

734 **DUET for extremely large datasets used in pre-training.** We can amortize the computational
735 cost of IF computation by pre-computing and storing them beforehand (App. A.4) in our paper’s
736 fine-tuning setting. However, the size of datasets used in pre-training could be extremely large, which
737 might still lead to large computational cost when computing IF scores of every data point in such
738 datasets. To make computation faster, we can adopt methods in (Koh & Liang, 2017) to approximate
739 hessian inversions when computing IF scores. We can also sample a smaller subset of data to compute
740 IF scores, before training a neural network (Jethani et al., 2022) to predict the IF scores of other data
741 points.

742 **Noisy feedback setting.** In some practical settings, the feedback from the unseen task is noisy. For
743 instance, user ratings have a variance even within the same user demographics. How does DUET fare
744 when the feedback from the unseen evaluation task is noisy? Fortunately, DUET is equally effective
745 even when feedback is noisy. Feedback noise becomes part of the observation noise (Sec. 3.3) under
746 the BO framework in DUET. In our experiments (Sec. 6.2), the evaluation task feedback is inherently
747 noisy since LLM responses are probabilistic in nature, but DUET still performs well empirically.

748 A.4 INFLUENCE FUNCTION AND ITS CALCULATIONS
749

750 Influence function (IF) (Koh & Liang, 2017) has been developed to study the influence of a single data
751 point on an ML model’s predictions. In this section we provide a summary of IF and its derivation.
752 The influence of a data point z on the loss of a test data point (or a set of test data points) z_{test} for an
753 ML model parameterized by θ is given by the closed-form expression:

$$754 \text{IF}_{z, z_{\text{test}}} = -\nabla_{\theta} L(z_{\text{test}}, \theta)^T H_{\theta}^{-1} \nabla_{\theta} L(z, \theta), \quad (6)$$

756 where L is the loss function of the ML model and H is the hessian of the ML model w.r.t. parameters
 757 θ . In short, a data point is deemed more "influential" in reducing the model loss on a test data point
 758 if it has a higher IF score. As such, IF scores have also become a popular method in selecting data
 759 points which are more helpful in training an ML model.

760 In our work, we segregated a validation dataset from each data domain's dataset, in which we use
 761 to derive the IF score of every training data point in that domain w.r.t. the validation dataset (after
 762 fine-tuning an LLM over the training data till convergence). Then, we normalize these IF scores (for
 763 data points in each data domain), allowing us to perform weighted random sampling at every BO
 764 iteration of our algorithm, obtaining a data subset of size n for a given data domain. This IF-weighted
 765 sampling is repeated for every data domain until we sample a dataset fulfilling the proposed mixing
 766 ratio at every BO iteration. Hence, the resulting data mixture contains more proportion of high-quality
 767 data points (based on IF scores). A summary of the IF-weighted sampling process for one data
 768 domain is given in Alg. 2. In our algorithm, we repeat this procedure for every data domain.

769 **Algorithm 2** IF-weighted sampling for **one data domain containing** dataset D

- 771 1: **Input:** number of data points n required for the given data domain (taken from the mixing
 772 ratio proposed at current iteration). Dataset $D = \{x_1, x_2, \dots, x_{|D|}\}$, Influence value of each data
 773 point in data domain dataset D : $\mathcal{I} \triangleq [I_1, I_2, \dots, I_{|D|}]$, small constant ϵ to avoid degenerate-case
 774 normalization.
- 775 2: Normalize the IF scores into probabilities: $\mathcal{I}_{\text{normalized}} \triangleq$
 776 $\left[\frac{I_1 + \min(\mathcal{I}) + \epsilon}{\sum \mathcal{I}}, \frac{I_2 + \min(\mathcal{I}) + \epsilon}{\sum \mathcal{I}}, \dots, \frac{I_{|D|} + \min(\mathcal{I}) + \epsilon}{\sum \mathcal{I}} \right]$
- 777 3: Perform weighed sampling from dataset D according to weights given by $\mathcal{I}_{\text{normalized}}$ n times.

779 **IF scores can be pre-computed and stored.** In addition, we just need to pre-compute the IF
 780 scores of every data point once before reusing them repeatedly at every BO iteration to perform
 781 IF-weighted sampling. This greatly improves our algorithm's efficiency and runtime, as compared to
 782 other methods (see next section) which requires us to perform expensive computation every iteration.
 783 We provide the computation runtime of calculating IF scores in App. C.1.

784

785 A.5 DISCUSSION OF USING OTHER DATA SELECTION METHODS TO SOLVE INNER
 786 OPTIMIZATION PROBLEM IN DUET

787 Data selection methods (Albalak et al., 2024; Guo et al., 2024; Wang et al., 2024b) have been used to
 788 retrieve a representative subset of data from larger datasets. We note that in our work different data
 789 selection methods can be interchanged to produce different estimators for the inner problem solution
 790 in line 4 and 5 of Algorithm 1. For example, instead of using the IF-driven estimator which performs
 791 weighted sampling based on each data point's IF scores, one could use LESS (Xia et al., 2024) to
 792 retrieve data subsets for the inner optimization problem. However, our experiments (Fig. 6) have
 793 shown that other data selection methods perform slightly worse than IF when used in DUET's inner
 794 loop. We speculate that this occurs for a few reasons.

795 Specifically, IF (Koh & Liang, 2017) is effective at identifying non-useful data (e.g., nonsensical text,
 796 text with lots of spelling mistakes, blur images) and so IF will down-weigh low-quality datapoints
 797 when we sample from that data domain. Doing so is effective in DUET's setting because these
 798 nonsensical training data are unlikely to be useful for any tasks, so their removal can boost the
 799 performance of the selected data mixture on the unseen task. While LESS contains a similar
 800 formulation as IF, it merely consider the gradient dot-products and ignores the hessian of the loss
 801 function (Koh & Liang, 2017) during computation. Hence, it does not contain as much information
 802 as IF.

803 In addition, diversity-driven methods (Wang et al., 2024b; Zhang et al., 2024) tend to select training
 804 data subsets that are "most representative" of the training data domain. However, from observation,
 805 they tend to keep nonsensical data points in the final data mixture, which is not as effective as IF,
 806 which down-samples these points. Also, representative data of a training domain might not be useful
 807 for an unseen task if the task is not related. Lastly, when calculating the data log-determinant, we
 808 need to project data into embedding space with an embedding model, and hence the effectiveness of
 809 the embedding model also affects the selection process. Effectiveness aside, diversity-driven methods
 are also dependent on the mixing ratio chosen at each iteration. Therefore, we need to recompute

810 the log-determinant (Wang et al., 2024b) or coresnet (Zhang et al., 2024) at every iteration. On the
 811 contrary, IF scores can be pre-computed and stored prior to running DUET.
 812

813 Therefore, different selection methods have different properties (above), but conceptually and empirically,
 814 we found IF to work better in our unseen task setting. Our ablation studies (Fig. 6) affirms our
 815 claim: using IF in DUET attains the highest performance as compared to selection methods such as
 816 LESS and log-determinant. We hope DUET can serve as a testbed for more advanced data-selection
 817 methods in the future.
 818

819 A.6 MORE DISCUSSION ON THE IF-DRIVEN ESTIMATOR

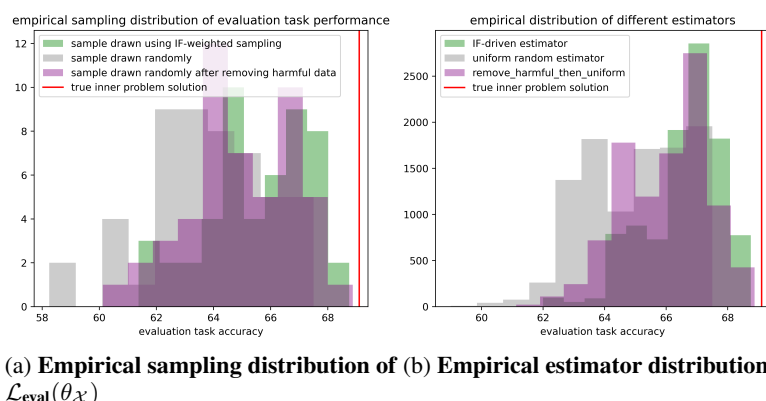
820 Here, we provide more justification behind our choice of the IF-driven estimator.
 821

822 **Why not take the data with the top-N IF scores instead of sampling?** One obvious alternative
 823 is to pick the data subset with the top IF scores (satisfying the given data ratio) or remove the
 824 datasubset with the lowest IF scores. We did not find this selection method effective in practice.
 825 Because IF-values are pre-computed and independent (App. A.4), we end up selecting the same few
 826 datapoints with top IF scores at every BO iteration in DUET. With the IF-weighted sampling, we
 827 select more diverse data points, yielding better data mixtures. This becomes more apparent when
 828 many data points have high IF scores and sampling provides us access to these data points at every
 829 iteration. Empirically, we also found that the deterministic approach performs worse (See DUET-RH
 830 in Sec. 6.2) than IF-weighted sampling.
 831

832 Performing weighted-sampling with IF-scores not only retains the benefits of using IF-scores (we
 833 outweigh higher quality data while still having access to data points with moderate IF-scores), but also
 834 allows us to exploit additional computational resources to reduce the estimation error by increasing
 835 the sampling size. For instance, Theorem 3.2 shows that higher sampling size reduces the inner
 836 problem estimation variance and bias. Intuitively, an LLM owner could exploit more compute to
 837 increase sampling size k and sample more data mixtures and reduce the estimation error at every BO
 838 iteration. These estimation error variances are also handled gracefully in the BO framework.
 839

840 In our experiments, we demonstrate that even with limited resource to sample and train an LLM once
 841 ($k = 1$), DUET still outperforms other baselines in our setting. In fact, Our ablation (Fig. 7) shows
 842 that increasing k results in a performance boost, showcasing the benefits of sampling in real-world
 843 settings (where computational resources are available to make multiple queries each BO step).
 844

845 A.7 EMPIRICAL DISTRIBUTIONS OF ESTIMATORS FROM DIFFERENT DATA SELECTION 846 METHODS



857 (a) **Empirical sampling distribution of (b) Empirical estimator distribution**
 858 $\mathcal{L}_{\text{eval}}(\theta_{\mathcal{X}})$

859 Figure 8: (a): Empirical distribution of evaluation task accuracy $\mathcal{L}_{\text{eval}}(\theta_{\mathcal{X}})$ from each data mixture
 860 sample \mathcal{X} (b): empirical distribution of the estimators introduced in Sec. 3.2. The **green histogram**
 861 is our method of performing IF-weighted sampling to obtain data mixtures. The **gray histogram** is
 862 simply randomly sampling data mixtures with no data selection methods. The **purple histogram** is the
 863 method of removing 20% of the data points with the lowest IF scores.
 864

We have introduced the IF-driven estimator in Sec. 3.2 to estimate the solution of the inner problem. The IF-driven estimator performs IF-weighted sampling on data points from each data domain to produce data mixture samples (Eq. 5) constrained to a data mixing ratio r . Each data mixture sample is then used to train/fine-tune an LLM before obtaining a feedback on how well it has performed on the unseen evaluation task. Hence, this feedback based on each data mixture sample is also a sampling distribution that we can empirically observe. Fig. 8a shows the sampling distribution of the evaluation task performance obtained from each data mixture. Empirically, we see that the negative of this distribution is similar to a truncated exponential distribution mentioned in Theorem 3.2 (We consider the negative of this random variable because our paper considers the evaluation task loss, but empirically we maximize the evaluation task accuracy). In addition, the truncated exponential distribution is appropriate because it implies the unseen evaluation task loss is upper bounded at $y_r^* + c$ for a non-negative constant c ; this is a reasonable assumption because many real-world feedbacks are bounded (e.g. user ratings).

We also plot the empirical distribution of the IF-driven estimator introduced in Eq. 5 in Fig. 8b. The distribution coincides with the estimator’s distribution (formally, $y_r^* + \epsilon$) introduced in Theorem 3.2. From the estimator’s distribution, we see that the IF-driven estimator (green histogram) has the lower bias and variance as compared to other estimators.

B PROOFS

B.1 PROOF OF THEOREM 3.1

Theorem 3.1. \mathcal{X}^* , the optimal set of data points from \mathcal{D} , is the solution of the original problem 2 iff $r^* = \text{ratio}(\mathcal{X}^*)$ is the optimal mixing ratio solution of the reparameterized problem:

$$\min_{r \in \mathbb{R}^n} \min_{\mathcal{X} \in S_r} \mathcal{L}_{\text{eval}}(\theta_{\mathcal{X}}), \quad (3)$$

where $S_r \triangleq \{\mathcal{X} : \mathcal{X} \in \mathcal{D}, \text{ratio}(\mathcal{X}) = r, |\mathcal{X}| = M\}$ and $\text{ratio}(\mathcal{X}) = r$ means that the data points in \mathcal{X} satisfies the mixing ratio $r \in \mathbb{R}^N$ from n data domains and $\|r\|_1 = 1$.

Proof. Theorem. 3.1 can be proven in two steps. First, we restate the theoretical results from (Chen et al., 2024b) in Lemma B.1. This Lemma reparameterizes any optimization problem ($\min_x f(x)$) (while retaining the solution set *exactly*) under some regular assumptions:

Lemma B.1. Let $x \in \mathbb{R}^d$ and $y \in \mathbb{R}^n$. Also, consider well-defined functions f over $\mathbb{R}^d \rightarrow \mathbb{R}$ and g over $\mathbb{R}^d \rightarrow \mathbb{R}^n$. Then x^* is a solution of $\arg \min_x f(x)$ if and only if $y^* = g(x^*)$ is a solution of the second optimization problem over domain $\{y \mid \exists x, g(x) = y\}$:

$$\begin{aligned} \min_y \min_x & f(x) \\ \text{s.t. } & g(x) = y \end{aligned}$$

The proof of Lemma B.1 can be found in Lemma C.1 of (Chen et al., 2024b). Next, we show that the objective function of problem 3 introduced in our optimization problem satisfies these assumptions, allowing us to apply the Lemma B.1 directly.

In our setting, we set $x \triangleq \mathcal{X}$, $f(x) \triangleq \mathcal{L}_{\text{eval}}(\theta_{\mathcal{X}})$ and $g(x) \triangleq \text{ratio}(\mathcal{X})$. We can see that both functions are well-defined, where for any chosen input \mathcal{X} , there certainly exists an observed evaluation task loss $\mathcal{L}_{\text{eval}}(\theta_{\mathcal{X}})$ and mixing ratio $\text{ratio}(\mathcal{X})$. Lastly, by setting $y \triangleq r$, our optimization problem in problem 3 is of the identical form of the optimization problem shown in Lemma B.1. Therefore, our reparameterization process is valid. \square

B.2 PROOF OF THEOREM 3.2

Theorem 3.2. Let $\{\mathcal{X}_1^{IF}, \dots, \mathcal{X}_k^{IF}\}$ be k data mixture samples drawn from S_r using IF-weighted sampling. Furthermore, assume each independent sample $\mathcal{L}_{\text{eval}}(\theta_{\mathcal{X}_i^{IF}})$ follows the shifted truncated

918 exponential distribution $y_r^* + \exp_t(\lambda, c)$, for $i = 1, 2, \dots, k$ where $\exp_t(\lambda, c)$ is a truncated exponential distribution governed by rate parameter λ and truncated at $c > 0$. Then, the IF-driven estimator 919 y_r^* defined in Eq. 5 is a random variable: $y_r^* + \epsilon$, where y_r^* is the true inner problem solution of Eq. 4 920 and ϵ is a random noise variable with probability density function (PDF): 921

$$923 \quad PDF_\epsilon(u) = \frac{\lambda k e^{-\lambda u}}{1 - e^{-\lambda c}} \left(\frac{e^{-\lambda u} - e^{-\lambda c}}{1 - e^{-\lambda c}} \right)^{k-1} \text{ on } u \in [0, c].$$

926 *Proof.* Let X_1, X_2, \dots, X_k be k samples randomly drawn from a sampling distribution and $X_{\min} =$
927 $\min\{X_1, X_2, \dots, X_k\}$. This scenario mirrors the setting in Theorem 3.2. Our goal is to derive
928 the distribution of X_{\min} and show that it is exactly the same as the distribution of \tilde{y}_r^* shown in the
929 Theorem 3.2.

930 If each random sample $X_i \sim \exp_t(\lambda, c)$, we first use a commonly known result (Chen et al., 2024b)
931 that the CDF of any truncated distribution on $[0, c]$ is $\frac{F(u) - F(0)}{F(c) - F(0)}$ where F is the CDF of the original
932 distribution. Also, we note that for the untruncated exponential distribution, $F(u) = 1 - e^{-\lambda u}$.
933 Hence, The CDF of X_{\min} is
934

$$936 \quad \text{cdf}_{(X_{\min})}(u) = 1 - \mathbb{P}(X_{\min} \geq u) \\ 937 \quad = 1 - \mathbb{P}(X_1 \geq u, X_2 \geq u, \dots, X_k \geq u) \\ 938 \quad = 1 - \left(1 - \frac{1 - e^{-\lambda u}}{1 - e^{-\lambda c}} \right)^k, \quad 0 \leq u \leq c.$$

941 and so the PDF of X_{\min} can be computed as
942

$$943 \quad \text{PDF}_{(X_{\min})}(u) = \frac{\partial}{\partial u} F_{(X_{\min})}(u) \\ 944 \quad = \frac{\lambda k e^{-\lambda u}}{1 - e^{-\lambda c}} \left(\frac{e^{-\lambda u} - e^{-\lambda c}}{1 - e^{-\lambda c}} \right)^{k-1}, \quad 0 \leq u \leq c.$$

948 In the original Theorem, each sample X_i follows the shifted truncated exponential distribution
949 $y_r^* + \exp_t(\lambda, c)$ where y_r^* is a constant. Hence, we can see that our estimator has the distribution of
950 $y_r^* + X_{\min}$ where X_{\min} has the PDF above. Hence, the Theorem is proven by setting the random
951 variable $\epsilon = X_{\min}$.
952

□

955 B.3 PROOF OF THEOREM 4.1

956 **Theorem 4.1.** *Let f be the outer problem objective defined in Sec. 3.3 with bounded RKHS norm:
957 $\|f\|_\kappa = \sqrt{\langle f, f \rangle_\kappa}$. Also, let our IF-driven estimator for the inner problem solution be governed by the
958 error distribution introduced in Theorem 3.2 with constant c and $\lambda = 1$. Let $A_{c,k} = \frac{c^2(1-e^{-c}-\frac{c}{2})^{k-1}}{(1-e^{-c})^k}$,
959 where k is a fixed predecided sampling size. Then, running DUET over f using the LCB acquisition
960 function found in (Chowdhury & Gopalan, 2017) at each BO iteration $t = 1, \dots, T$ yields the
961 following **attained average regret** (Chen et al., 2024b) upper bound with probability at least $1 - \delta$:*
962

$$964 \quad \lim_{T \rightarrow \infty} \frac{\tilde{R}_T}{T} \leq \frac{6(\sqrt[4]{\delta} + \sqrt{k})}{\sqrt[4]{\delta}k} + 2A_{c,k} + \frac{\sqrt{2A_{c,k}}}{\sqrt[4]{\delta}}.$$

967 *Proof.* We provide the proof of the sub-linear \tilde{R}_T growth of DUET in Theorem 4.1 by establishing
968 upper bounds of $|\mu_t(x) - f(x)|$ and ϵ_t separately at each BO iteration t and use the independence
969 rule to bound their sum. To do so, we introduce the following two Lemmas.
970

971 Our first Lemma is taken from known literature on Kernelized Bandits (Chowdhury & Gopalan,
972 2017) and provides the upper bound on difference between $f(x_t)$ and $\mu_t(x)$ at each BO iteration t .

972 **Lemma B.2.** Let $\|f\|_\kappa = \sqrt{\langle f, f \rangle_\kappa} \leq B$. Also, assume that the observation noise associated with
 973 each BO iteration is R -sub-Gaussian with $R > 0$. Then with probability at least $1 - \delta$, the following
 974 holds for BO iteration $t \leq T$:

$$975 \quad 976 \quad |\mu_t(x) - f(x)| \leq \left(B + R\sqrt{2(\gamma_t + 1 + \ln(1/\delta))} \right) \sigma_t(x) \quad (7)$$

978 where γ_t is the maximum information gain after t observations and $\mu_t(x), \sigma_t^2(x)$ are mean and
 979 variance of posterior distribution of GP defined in Equation 1, with $\lambda = 1 + 2/T$.

981 Our second Lemma attempts to bound the expectation and variance of ϵ_t , the non-negative observation
 982 noise (in our case, it corresponds to the estimation error involved in solving the inner problem) at
 983 each BO iteration t . These expectation and variance will be used later to bound our cumulative regret.

985 **Lemma B.3.** Let each observation noise ϵ_t of BO iteration t follow the same probability dis-
 986 tribution as ϵ defined in Theorem 3.2 with sampling size k probability density function $f_{\epsilon_t}(u) =$
 987 $\frac{\lambda k e^{-\lambda u}}{1 - e^{-\lambda c}} \left(\frac{e^{-\lambda u} - e^{-\lambda c}}{1 - e^{-\lambda c}} \right)^{k-1}$ with $0 < c \leq 1$, $\lambda = 1$ and $u \in [0, c]$, then $\mathbb{E}(\epsilon_t) \leq \frac{6}{k} + \frac{2c^2((1-e^{-c}) - \frac{c}{2})^{k-1}}{(1-e^{-c})^k}$
 988 and $\text{Var}(\epsilon_t) \leq \mathbb{E}(\epsilon_t)$.

990 *Proof.* For $\lambda = 1$, we have that $f_{\epsilon_t}(u) = \frac{ke^{-u}}{1-e^{-c}} \left(\frac{e^{-u} - e^{-c}}{1 - e^{-c}} \right)^{k-1}$ with $0 < c < 1$ and $u \in [0, c]$.
 991 Then, the expectation:

$$\begin{aligned} 995 \quad \mathbb{E}(\epsilon_t) &= \int_0^c u f_{\epsilon_t}(u) du \\ 996 \quad &= \int_0^c \frac{uke^{-u}}{1 - e^{-c}} \left(\frac{e^{-u} - e^{-c}}{1 - e^{-c}} \right)^{k-1} du \\ 997 \quad &= \frac{k}{(1 - e^{-c})^k} \int_0^c ue^{-u} (e^{-u} - e^{-c})^{k-1} du \\ 998 \quad &\stackrel{(1)}{\leq} \frac{k}{(1 - e^{-c})^k} \int_0^c u (e^{-u} - e^{-c})^{k-1} du \\ 999 \quad &\stackrel{(2)}{\leq} \frac{k}{(1 - e^{-c})^k} \int_0^c u \left(\left(1 - \frac{u}{2}\right) - e^{-c} \right)^{k-1} du \\ 1000 \quad &\stackrel{(3)}{\leq} \frac{k}{(1 - e^{-c})^k} \left(\frac{(u - 2(1 - e^{-c}))((1 - e^{-c}) - \frac{u}{2})^{k-1}(2(1 - e^{-c}) + (k-1)u + u)}{k(k+1)} \right) \Big|_{u=0}^{u=c} \\ 1001 \quad &\stackrel{(4)}{=} \frac{1}{(1 - e^{-c})^k} \left(\frac{(c - 2(1 - e^{-c}))((1 - e^{-c}) - \frac{c}{2})^{k-1}(2(1 - e^{-c}) + kc) + 4(1 - e^{-c})^{k+1}}{k+1} \right) \\ 1002 \quad &\stackrel{(5)}{\leq} \frac{4(1 - e^{-c})^{k+1}}{(k+1)(1 - e^{-c})^k} + \frac{2kc^2((1 - e^{-c}) - \frac{c}{2})^{k-1}}{(k+1)(1 - e^{-c})^k} + \frac{2((1 - e^{-c}) - \frac{c}{2})^{k-1}(1 - e^{-c})}{(k+1)(1 - e^{-c})^k} \\ 1003 \quad &\stackrel{(6)}{\leq} \frac{6}{k} + \frac{2c^2((1 - e^{-c}) - \frac{c}{2})^{k-1}}{(1 - e^{-c})^k} \end{aligned} \quad (8)$$

1019 where $\stackrel{(1)}{\leq}$ makes use of the fact that $e^{-\lambda u} \leq 1$ for $u \in [0, c]$ with $c > 0$, $\stackrel{(2)}{\leq}$ uses the inequality
 1020 $e^{-u} \leq 1 - \frac{u}{2}$ for $u \in [0, c]$, and $c \leq 1$, $\stackrel{(3)}{=}$ uses the fact that $e^{-\lambda c} < 1$, $\stackrel{(4)}{=}$ is derived by solving
 1021 the definite integral by parts and substitution and $\stackrel{(4)}{=}$ simplifies the upper bound with algebraic
 1022 manipulation.

1023 Next, the upper bound of the variance of ϵ_t can be derived by

1026

1027

1028

1029

1030

1031

1032

1033

1034

1035

1036

1037

1038

1039

1040

1041

1042

1043

1044

1045

1046

1047

1048

1049

1050

1051

1052

1053

1054

1055

1056

1057

1058

1059

1060

1061

1062

1063

1064

1065

1066

1067

1068

1069

1070

1071

1072

1073

1074

1075

1076

1077

1078

1079

$$\begin{aligned}
\text{Var}(\epsilon_t) &= \int_0^c u^2 f_{\epsilon_t}(u) du \\
&\stackrel{(1)}{\leq} c \int_0^c u f_{\epsilon_t}(u) du \\
&\stackrel{(2)}{\leq} \int_0^c u f_{\epsilon_t}(u) du \\
&= \mathbb{E}(\epsilon_t)
\end{aligned} \tag{9}$$

where $\stackrel{(1)}{\leq}$ makes use of the fact that ϵ_t lies in $[0, c]$ and $\stackrel{(2)}{\leq}$ makes use of the fact that $0 < c \leq 1$. This completes the proof on the bounds on $\mathbb{E}(\epsilon_t)$ and $\text{Var}(\epsilon_t)$. \square

Next, we observe that x_t at each BO iteration t is chosen via the IGP-LCB acquisition function (i.e., $x_t = \arg \min_x \mu_{t-1}(x) - \beta_t \sigma_{t-1}(x)$ and $\beta_t = B + R\sqrt{2(\gamma_{t-1} + 1 + \ln(1/\delta_1))}$ where the observation noise associated with each BO iteration is R -sub Gaussian). Thus, we can see that at each iteration $t \geq 1$, we have $-\mu_{t-1}(x_t) + \beta_t \sigma_{t-1}(x_t) \geq -\mu_{t-1}(x^*) + \beta_t \sigma_{t-1}(x^*)$. It then follows that for all $t \geq 1$ and with probability at least $1 - \delta_1$,

$$\begin{aligned}
|f(x_t) - f(x^*)| &\stackrel{(1)}{\leq} f(x_t) - \mu_{t-1}(x^*) - \beta_t \sigma_{t-1}(x^*) \\
&\stackrel{(2)}{\leq} f(x_t) - \mu_{t-1}(x_t) + \beta_t \sigma_{t-1}(x_t) \\
&\leq \beta_t \sigma_{t-1}(x_t) + |\mu_{t-1}(x_t) - f(x_t)| \\
&\leq 2\beta_t \sigma_{t-1}(x_t)
\end{aligned} \tag{10}$$

Therefore, by setting $\delta_1 = \delta_2 = \sqrt{\delta}$, it follows that with probability $1 - \delta$ (this follows by rule of independence applied to the upper bound of events $\sum_{t=1}^T |f(x_t) - f(x^*)|$ and $\sum_{t=1}^T \epsilon_t$) that our **attained cumulative regret** can be bounded as

$$\begin{aligned}
\tilde{R}_T &= \sum_{t=1}^T |\tilde{y}_t - f(x^*)| \\
&= \sum_{t=1}^T |f(x_t) - f(x^*) + \epsilon_t| \\
&\stackrel{(1)}{=} \sum_{t=1}^T |f(x_t) - f(x^*)| + \sum_{t=1}^T \epsilon_t \\
&\stackrel{(2)}{\leq} 2\beta_T \sum_{t=1}^T \sigma_{t-1}(x_t) + \sum_{t=1}^T \epsilon_t \\
&\stackrel{(3)}{=} 2 \left(B + R\sqrt{2(\gamma_T + 1 + \ln(1/\sqrt{\delta}))} \right) \sum_{t=1}^T \sigma_{t-1}(x_t) + \sum_{t=1}^T \epsilon_t \\
&\stackrel{(4)}{\leq} 2 \left(B + R\sqrt{2(\gamma_T + 1 + \ln(1/\sqrt{\delta}))} \right) \sum_{t=1}^T \sigma_{t-1}(x_t) + \sum_{t=1}^T \mathbb{E}(\epsilon_t) + \sum_{t=1}^T \sqrt{\frac{\text{Var}(\epsilon_t)}{\delta_2}} \\
&\stackrel{(5)}{=} 2 \left(B + R\sqrt{2(\gamma_T + 1 + \ln(1/\sqrt{\delta}))} \right) O(\sqrt{T\gamma_T}) + \sum_{t=1}^T \mathbb{E}(\epsilon_t) + \sum_{t=1}^T \sqrt{\frac{\text{Var}(\epsilon_t)}{\delta_2}} \\
&= O \left(\sqrt{T} (B\sqrt{\gamma_T} + R\gamma_T) \right) + \sum_{t=1}^T \mathbb{E}(\epsilon_t) + \sum_{t=1}^T \sqrt{\frac{\text{Var}(\epsilon_t)}{\delta_2}} \\
&\stackrel{(6)}{=} O \left(\sqrt{T} (B\sqrt{\gamma_T} + \frac{c^2 \gamma_T}{4}) \right) + \sum_{t=1}^T \mathbb{E}(\epsilon_t) + \sum_{t=1}^T \sqrt{\frac{\text{Var}(\epsilon_t)}{\delta_2}}
\end{aligned} \tag{11}$$

1080 where we have followed the attained cumulative regret proof in (Chen et al., 2024b) closely and used
 1081 the following facts:
 1082

- 1084 • $\stackrel{(1)}{=}$ uses the fact that ϵ_t is non-negative in our problem setting (Theorem. 3.2).
- 1085 • $\stackrel{(2)}{\leq}$ is derived from Eq. equation 10.
- 1086 • $\stackrel{(3)}{=}$ uses the definition of β_T in IGP-LCB acquisition function (Chowdhury & Gopalan, 2017)
 1087 w.r.t. $\delta_1 = \sqrt{\delta}$
- 1088 • $\stackrel{(4)}{\leq}$ uses Chebyshev's inequality over ϵ_t with probability at least $1 - \delta_2$.
- 1089 • $\stackrel{(5)}{=}$ uses $\sum_{t=1}^T \sigma_{t-1}(x_t) \leq O(\sqrt{T\gamma_T})$ as shown in **Lemma 4** by Chowdhury & Gopalan
 1090 (Chowdhury & Gopalan, 2017).
- 1091 • $\stackrel{(6)}{=}$ uses the fact that ϵ_t is bounded on $[0, c]$ and all bounded random variables are R-sub-
 1092 Gaussian with $R = \frac{c^2}{4}$ (Arbel et al., 2019).

1093 Next, we need to derive the upper bound of $\sum_{t=1}^T \mathbb{E}(\epsilon_t) + \sum_{t=1}^T \sqrt{\frac{\text{Var}(\epsilon_t)}{\delta_2}}$ w.r.t. T . This can be done
 1094 by using the upper bound of the expectation and variance of ϵ_t proven in Lemma B.3:
 1095

$$\begin{aligned} 1103 \sum_{t=1}^T \mathbb{E}(\epsilon_t) + \sum_{t=1}^T \sqrt{\frac{\text{Var}(\epsilon_t)}{\delta_2}} &\stackrel{(1)}{\leq} \sum_{t=1}^T \left(\frac{6}{k} + \frac{2c^2((1-e^{-c}) - \frac{c}{2})^{k-1}}{(1-e^{-c})^k} \right) + \sum_{t=1}^T \sqrt{\frac{6}{\delta_2 k} + \frac{2c^2((1-e^{-c}) - \frac{c}{2})^{k-1}}{\delta_2(1-e^{-c})^k}} \\ 1104 &= \frac{6T}{k} + \frac{2Tc^2((1-e^{-c}) - \frac{c}{2})^{k-1}}{(1-e^{-c})^k} + T \sqrt{\frac{6}{\delta_2 k} + \frac{2c^2((1-e^{-c}) - \frac{c}{2})^{k-1}}{\delta_2(1-e^{-c})^k}} \end{aligned} \quad (12)$$

1110 where $\stackrel{(1)}{\leq}$ uses Lemma B.3 directly.

1111 Then, it follows from Eq. 11 and 12 that with probability $1 - \delta$ and $\delta_2 = \sqrt{\delta}$, the **attained cumulative**
 1112 **regret** \tilde{R}_T at iteration T is upper bounded by:
 1113

$$1116 \tilde{R}_T \leq O \left(\sqrt{T} \left(B \sqrt{\gamma_T} + \frac{c^2 \gamma_T}{4} \right) \right) + \frac{6T}{k} + \frac{2Tc^2((1-e^{-c}) - \frac{c}{2})^{k-1}}{(1-e^{-c})^k} + T \sqrt{\frac{6}{\delta_2 k} + \frac{2c^2((1-e^{-c}) - \frac{c}{2})^{k-1}}{\delta_2(1-e^{-c})^k}} \quad (13)$$

1120 Finally we set $A_{c,k} = \frac{c^2(1-e^{-c} - \frac{c}{2})^{k-1}}{(1-e^{-c})^k}$. As $T \rightarrow \infty$, with probability $1 - \delta$ and $\delta_2 = \sqrt{\delta}$, the attained
 1121 *average* regret converges to:
 1122

$$\begin{aligned} 1123 \lim_{T \rightarrow \infty} \frac{\tilde{R}_T}{T} &\stackrel{(1)}{\leq} \frac{6}{k} + \frac{2((1-e^{-c}) - \frac{c}{2})^{k-1}}{(1-e^{-c})^k} + \sqrt{\frac{6}{\delta_2 k} + \frac{2((1-e^{-c}) - \frac{c}{2})^{k-1}}{\delta_2(1-e^{-c})^k}} \\ 1124 &\stackrel{(2)}{\leq} \frac{6}{k} + \sqrt{\frac{6}{\delta_2 k}} + 2A_{c,k} + \sqrt{\frac{2A_{c,k}}{\delta_2}} \\ 1125 &\leq \frac{6(\sqrt[4]{\delta} + \sqrt{k})}{\sqrt[4]{\delta} k} + 2A_{c,k} + \sqrt{\frac{2A_{c,k}}{\delta_2}} \end{aligned} \quad (14)$$

1131 where $\stackrel{(1)}{\leq}$ divides Eq. 13 by T throughout, eliminating the O expression and $\stackrel{(2)}{\leq}$ uses the substitution of
 1132 $A_{c,k}$ and triangle inequality. This completes our proof for the attained average regret in Theorem 4.1.
 1133 \square

1134
1135

B.4 EXTENDING THEORETICAL ANALYSIS BASED ON DIFFERENT DATA SELECTION METHODS

1136
1137
1138

Readers might be interested in how different data selection methods used to create different estimators affect our theoretical analysis. Here, we provide details on how one could replicate our paper’s theoretical analysis to different estimators.

1139
1140
1141
1142
1143
1144
1145
1146

Step 1. Establish the sampling distribution of $\mathcal{L}_{\text{eval}}(\theta_{\mathcal{X}})$. Using a particular data selection method, one obtains k data mixture samples $\{\mathcal{X}_1, \dots, \mathcal{X}_k\}$ (in our paper, these samples are obtained via weighted sampling based on each data point’s IF scores). Then, one trains an LLM for each data mixture and obtain the evaluation task loss for each resulting LLM, yielding $\{\mathcal{L}_{\text{eval}}(\theta_{\mathcal{X}_1}), \dots, \mathcal{L}_{\text{eval}}(\theta_{\mathcal{X}_k})\}$. From this set, one can empirically derive the sampling distribution of each sample $\mathcal{L}_{\text{eval}}(\theta_{\mathcal{X}_i})$. In Theorem 3.2, we assumed that each sample $\mathcal{L}_{\text{eval}}(\theta_{\mathcal{X}_i})$ follows the truncated exponential distribution. However, different data selection methods would certainly lead to different empirical sampling distributions.

1147
1148
1149
1150
1151
1152
1153
1154
1155
1156

Step 2. Derive an estimator’s empirical distribution. Next, we need to theoretically derive the 1st-order statistic (Arnold et al., 2008) of the empirical sampling distribution from Step 1, since we use the 1st-order statistic as our estimator. The procedure to do so is shown in App. B.2 and uses a fairly standard procedure to derive the distribution of order statistics. For subsequent analysis to be tractable, the PDF of the 1st-order statistic should have a closed form (hence, a simpler sampling distribution in Step 1 is preferred). More importantly, the estimator’s empirical distribution **should be R-sub-gaussian** for a fixed $R > 0$. This is because for the regret-analysis proof in Eq. 11 to hold true, the observation noise in the BO process should be R-sub-Gaussian. Fortunately, a large family of random distributions, including our IF-driven estimator introduced in this paper, are all R-sub-Gaussian (e.g., exponential family, all bounded random variables).

1157
1158

Step 3. Derive the upper bound of estimator’s expectation and variance. Next, we derive the upper bound of the 1st-order statistic’s expectation and variance as shown in Lemma. B.3.

1159
1160
1161
1162
1163
1164

Step 4. Derive attainable cumulative regret. Lastly, we analyze the convergence rate of our algorithm using the growth of *attained cumulative regret* (Chen et al., 2024b) $\tilde{R}_T = \sum_{t=1}^T |\tilde{y}_{r_t}^* - f(r_t)| = \sum_{t=1}^T |f(r^*) + \epsilon_t - f(r_t)|$ for T BO iterations. Since the error term ϵ_t has the same expectation and variance of our estimator, we can use the results from Step 3 to derive our regret bound (as shown in Eq. 11).

1165

C ADDITIONAL EXPERIMENTAL RESULTS AND DISCUSSIONS

1166
1167
1168
1169

C.1 ADDITIONAL DETAILS ON EXPERIMENTAL SETUP

1170
1171
1172
1173
1174
1175
1176
1177
1178
1179
1180
1181
1182
1183
1184

In this section, we provide additional details in our experiments for ease of reproduceability. Throughout our experiments, we used the SE kernel with lengthscale parameters learned from historical observations via maximum-likelihood (Williams & Rasmussen, 2006). In our LCB acquisition function (Greenhill et al., 2020), we set $\beta_t = 0.5$ (see Alg. 1) throughout our experiments. Furthermore, we need to perform constrained BO (Gardner et al., 2014) in our experiments because the inputs to our optimization problem is a data mixing ratio r whose sum of entries is constrained to 1. BoTorch allows us to implement such constraints (botorch.org/docs/constraints) easily. All evaluation for language tasks is done on **llm-harness** (Gao et al., 2024) with default 3-shot settings with no chain-of-thought or special prompting techniques. Hence, it is possible some of our paper’s results differ from those reported in other papers (due to different prompting and inference settings). However, our paper’s emphasis is on improving the LLM’s performance with a few rounds refinement on the training data mixture. Hence, we expect DUET to work well even in other inference settings. We treat the evaluation results on llm-harness as the feedback observed in our problem setting. For methods (e.g., uniform mixture, LESS, DoReMi) which do not use feedback, we repeat them 10 times to ensure fairness in comparison with DUET and show the best LLM performance in our results.

1185
1186
1187

To train the LLM, we used a LoRA (Hu et al., 2021) rank of 128 and the Adam optimizer (Kingma & Ba, 2017) with initial learning rate of 1e5. The specific hyperparameters surrounding our optimizers can be found in our code, which we have released. Each iteration of model fine-tuning is done in 1 epoch on a L40 Nvidia GPU and takes approximately an hour. So, performing 10 BO iterations take

1188 10 hours to run. In reality, the optimization process (all 10 iterations) will be carried out over a long
 1189 span of time (e.g., weeks, or even months) as part of the LLM deployment life-cycle. So this is a
 1190 reasonable amount of compute time.

1191 **IF computation.** To derive the IF scores of our training data, we remove 10% of the training data
 1192 from each data domain and treat it as the validation set. Then, we fine-tune a separate LLM for each
 1193 data domain (using the same setting as above and the same model type as that in our experiments),
 1194 before deriving the IF score of every data point from each data domain based on the converged LLM
 1195 and the validation dataset. Using 4 Nvidia L40 GPUS, we were able to compute the IF scores of
 1196 TriviaQA (containing around 170k data points) in around 2-3 hours with the torch- influence library
 1197 (<https://github.com/alstonlo/torch-influence>). Smaller datasets required even
 1198 shorter computation time. Certainly, these runtimes are reasonable in practical settings, since we only
 1199 need to compute the IF scores once and store them before running DUET.

1200 **Other data selection methods.** We can also use other data selection methods in DUET’s inner loop.
 1201 For instance, LESS (Xia et al., 2024) and TracIn (Pruthi et al., 2020) uses around 4-5 hours to build a
 1202 data-gradient store. On the other hand, diversity-driven selection techniques (Wang et al., 2024b)
 1203 are usually more computationally expensive, taking more than 30 hours to select the top 10000 data
 1204 points.

1206 C.2 COMPARISON WITH OTHER BASELINES

1207 One alternative baseline is to simply fine-tune the LLM on a training dataset for multiple more training
 1208 tokens (and epoch) and compare it with DUET. In Table 1, we fine-tuned Llama-3-8b-Instruct
 1209 for more epochs and training tokens on each training domain and evaluated on our evaluation task.
 1210 The results show that DUET-IF attains better results because it can exploit the feedback from the task.

1213 Table 1: Performance of models trained on different datasets across evaluation tasks.
 1214

1215 Train ↓ Eval. →	1216 TruthfulQA	1217 gsm8k	1218 PubmedQA+HeadQA	1219 Commonsense+TriviaQA
1220 Wikitext	42.8	70.4	40.6	59.9
1221 gsm8k	47.2	86.1	43.3	64.1
1222 Pubmed	43.3	71.5	49.3	58.4
1223 HeadQA	45.0	75.2	50.2	60.0
1224 SciQ	45.6	75.6	44.6	63.4
1225 TruthfulQA	59.0	74.0	43.8	61.0
Hellaswag	46.1	72.1	43.2	60.4
CommonsenseQA	50.1	73.3	47.2	65.8
TriviaQA	51.2	70.1	48.1	66.5
DUET-IF (ours)	59.8	84.2	52.4	69.6

1226
 1227 Next, we compared DUET (paired with different data selection methods) with a variety of naive
 1228 baselines. **Aioli** (Chen et al., 2024a), **Multi-Fid** (Yen et al., 2025) are two baselines that use domain
 1229 reweighting and multi-fidelity BO to optimize data mixtures. **IF** just picks the top $M = 20000$
 1230 datapoints with the highest influence scores. **Random** just selects a random subset of data, but we
 1231 subjected it to more training epochs and $M = 50000$ data points to ensure equal compute comparison.
 1232

1233
 1234
 1235
 1236
 1237
 1238
 1239
 1240
 1241

Table 2: Performance of other baselines across evaluation tasks.

Other baselines	TruthfulQA	gsm8k	PQA+HQA	Commonsense, TriviaQA
Aioli (Chen et al., 2024a)	51.1 \pm 0.7	76.5 \pm 1.2	48.8 \pm 0.5	63.7 \pm 1.0
Multi-Fid (Yen et al., 2025)	52.8 \pm 0.9	73.9 \pm 1.3	47.2 \pm 0.6	65.2 \pm 0.8
ODM (Albalak et al., 2023a)	46.1 \pm 1.1	77.3 \pm 0.4	45.8 \pm 1.2	60.1 \pm 0.7
IF only	50.8 \pm 0.5	76.9 \pm 0.8	47.7 \pm 0.9	57.8 \pm 0.6
Random	49.3 \pm 0.8	64.3 \pm 1.4	41.2 \pm 0.7	57.3 \pm 1.0
Uniform + more training tokens	51.6 \pm 0.8	64.4 \pm 1.3	44.5 \pm 1.2	59.2 \pm 1.6
DUET-IF (ours)	59.8\pm0.6	84.2\pm1.1	52.4\pm0.9	69.6\pm0.8
DUET-LESS (ours)	58.7\pm1.0	80.5\pm0.7	50.8\pm0.9	67.6\pm1.3

C.3 ADDITIONAL EXPERIMENTAL RESULTS WITH $\text{Qwen2.5-7B-Instruct}$

We repeated our experiments with $\text{Qwen2.5-7B-Instruct}$ in Fig. 9 and observe that DUET still can optimize data mixtures better than other baselines. This indicates that the effectiveness of DUET is independent of the model choice. Hence, we expect DUET to work well for other models as well.

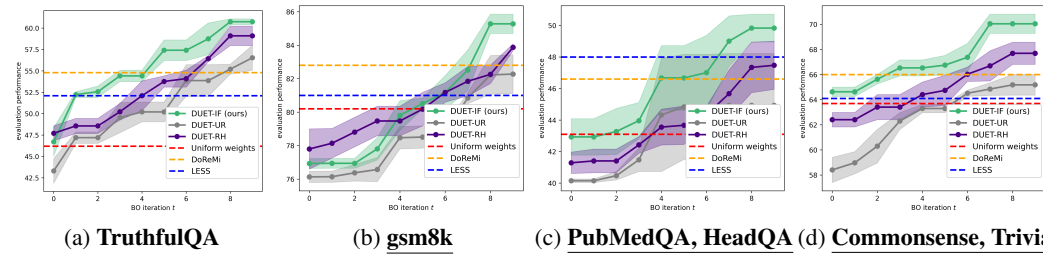


Figure 9: Results on unseen LLM evaluation task domains over 10 iterations (higher is better) for $\text{Qwen2.5-7b-Instruct}$. The subcaption indicates the evaluation domain. **Underlined evaluation tasks are more difficult** because the evaluation task domains are removed from the training data (i.e., OOD).

C.4 MIXING RATIO FOUND BY DUET

We also present the mixing ratio found by DUET for our experiments after 10 BO iterations. The column title denotes the evaluation task. When the unseen task is in-domain (**TruthfulQA**), DUET automatically finds that **TruthfulQA** is relevant training domain and places more weights on it. For OOD cases, DUET automatically finds relevant training domains as well. For example, even though we do not have **gsm8k** data for training, DUET automatically finds data from **wikitext** and **sciq** more relevant in improving the performance of the trained LLM.

Table 3: Mixing ratio found by DUET in our $\text{Llama-3-8b-Instruct}$ experiments after 10 BO iterations. The column indicates the unseen task domain, in the same setting and order as those found in our main experiments (Fig. 4). **NA** indicates the respective domain was not included in the training data.

Domains	TruthfulQA	gsm8k	PubMedQA, HeadQA	CommonsenseQA, TriviaQA
Commonsense	3	7	11	NA
<u>gsm8k</u>	0	NA	0	10
headqa	0	0	NA	0
hellaswag	0	1	0	28
pubmedqa	0	1	NA	0
sciq	2	38	34	22
triviaqa	3	12	19	NA
wikitext	8	41	30	22
TruthfulQA	84	1	6	18

1296 **D REBUTTAL ADDITIONS**
 1297

1298 **D.1 EXTENSION AND ADDITIONAL RESULTS ON FULL-PARAMETER FINETUNING OF LLMs**
 1299

1300 While it is too computationally expensive to perform large-scale pre-training *from scratch* for now,
 1301 we have performed additional experiments on **continual, full-parameter training** on 8B and 14B
 1302 models (in contrast to LoRA fine-tuning used in our paper). We performed these experiments on the
 1303 same setting (but we had to increase the training epoch to 3 for full-parameter training to converge
 1304 better) as in Fig.4(a) and 4(b) and show the best LLM performance achieved in 10 BO iterations.

Model Method	DUET-IF	DUET w/o IF	LESS
Llama-3-8B-Instruct	64.3 ± 0.8	60.1 ± 1.1	51.7 ± 0.7
Qwen3-14B	73.5 ± 0.6	70.1 ± 0.9	63.2 ± 1.0

1309 Table 4: Performance gain on TruthfulQA.
 1310

Model Method	DUET-IF	DUET w/o IF	LESS
Llama-3-8B-Instruct	85.1 ± 0.4	81.0 ± 0.7	74.4 ± 0.4
Qwen3-14B	88.6 ± 0.6	84.1 ± 0.9	80.2 ± 0.8

1315 Table 5: Performance gain on gsm8k (OOD).
 1316

1317 The results are generally consistent with our paper’s finding on LLM LoRA fine-tuning, and DUET
 1318 with IF performs better than its baselines. We will include this into the revised manuscript. We hope
 1319 these additional results suggest that our approach is equally feasible for full-parameter fine-tuning.

1320 One noteworthy point is that while computing IF scores for larger models is more expensive (i.e.,
 1321 computational cost scales with number of model parameters [1]), a practical approach is to use a
 1322 smaller surrogate model to compute the IF scores, which reduces the computational time. We used
 1323 the same set of IF-scores computed from the LoRA parameters here. If computational budget is a
 1324 concern, we can also free to use less expensive data selection methods in DUET’s inner loop (as
 1325 elaborated in Sec. 3.2 of our paper) with some performance-cost tradeoff.

1326 **D.2 DISCUSSION ON COMPUTATION AND MEMORY OVERHEAD OF DUET**
 1327

1328 Here, we provide a discussion of DUET-IF’s computation and memory overhead.
 1329

1330 **D.2.1 COMPUTATION OVERHEAD OF BO IN DUET**
 1331

1332 Let T denote the number of Bayesian Optimization (BO) iterations and n denote the dimension of
 1333 the data mixture (i.e., the number of training domains). In practice, the dominant cost of DUET
 1334 comes from fine-tuning the LLM T times, since BO requires multiple function evaluations (Frazier,
 1335 2018). This allows BO to exploit feedback from the unseen evaluation task and avoid brute-force
 1336 enumeration of all possible mixture ratios.

1337 Beyond LLM fine-tuning, BO incurs additional computational overhead. When using a Gaussian
 1338 Process (GP) surrogate, the primary cost arises from inverting the $T \times T$ kernel matrix when re-
 1339 estimating GP hyperparameters using maximum likelihood (see Eq. (5.8) in (Williams & Rasmussen,
 1340 2006)). This is typically performed using a Cholesky decomposition, which costs $\mathcal{O}(T^3)$.

1341 Next, optimizing the acquisition function at each iteration typically requires gradient-based opti-
 1342 mization. For the UCB acquisition function used in our work, computing gradients of the GP mean
 1343 and standard deviation incurs $\mathcal{O}((nT + nT^2)c)$ operations, where $\mathcal{O}(nT)$ comes from differentiat-
 1344 ing $\mu(x_{\text{candidate}})$, $\mathcal{O}(nT^2)$ from differentiating $\sigma(x_{\text{candidate}})$, and c is the number of restarts used in
 1345 acquisition optimization (see `botorch` acquisition optimization documentation).

1346 **(A)** Putting these together, the total BO compute at iteration T is:
 1347

$$\mathcal{O}(T^3) + \mathcal{O}((nT + nT^2)c) = \mathcal{O}(T^3),$$

1348 since typically $n \ll t$. Summing over from the first iteration yields the same $\mathcal{O}(T^3)$ complexity
 1349 because Cholesky updates allow reuse of factorizations, avoiding full recomputation at each iteration.

1350
1351

D.2.2 COMPUTATION OVERHEAD OF IF SCORES IN DUET-IF

1352
1353

When DUET is combined with data selection methods such as Influence Functions (IF), additional compute costs arise.

1354
1355
1356
1357
1358
1359

Influence Scores. Given N datapoints and p trainable model parameters (in other paper, p is the number of parameters in the model LoRA), direct computation of influence scores requires $\mathcal{O}(Np^2 + p^3)$ operations (Koh & Liang, 2017). However, stochastic estimation techniques (Sec. 3 in (Koh & Liang, 2017)) reduce this to $\mathcal{O}(Np)$. Importantly, IF scores only need to be computed once and can be reused across BO iterations.

1360
1361
1362
1363

Other Data Selection Methods. Different data selection strategies incur different costs, but these are typically amortized since they are computed once. For example, LESS incurs $\mathcal{O}(Nbp)$ operations, where b is the number of checkpoints used (Xia et al., 2024).

1364

Putting **(A)** and **(B)** together, the joint compute cost of DUET-IF is:

1365
1366

$$\mathcal{O}(T^3 + Np).$$

1367
1368

D.2.3 MEMORY OVERHEAD

1369
1370
1371
1372

BO alone requires $\mathcal{O}(T^2)$ memory to store the $T \times T$ kernel matrix. During IF computation, we require $\mathcal{O}(p)$ memory to store parameter gradients; the Hessian H need not be stored explicitly, as Hessian–vector products can be computed efficiently using conjugate gradient or stochastic methods (Koh & Liang, 2017). After computation, storing the IF scores requires $\mathcal{O}(N)$ memory.

1373

Thus, DUET-IF has a total memory overhead of:

1374
1375

$$\mathcal{O}(T^2 + p).$$

1376
1377

Additionally, because DUET fine-tunes an LLM using different data mixtures across BO iterations, we maintain a copy of the best-performing LoRA adaptor throughout the optimization.

1378
1379

CONCLUSION

1380

In summary, the computation overhead of DUET-IF is:

1381
1382
1383

$$\mathcal{O}(T^3) + \mathcal{O}(Np),$$

1384

where $\mathcal{O}(Np)$ can be precomputed before optimization and the memory overhead is:

1385
1386

$$\mathcal{O}(T^2 + p).$$

1387
1388

D.3 MORE DETAILS ON MIXING RATIO FOUND

1389
1390
1391
1392
1393
1394
1395
1396
1397
1398
1399
1400

↓ Domains → Iterations	1	2	3	4	5	6	7	8	9	10	DoReMi
commonsenseQA	11	0	0	11	28	0	11	80	3	0	14
gsm8k	11	0	0	9	0	0	10	16	0	90	4
headQA	11	0	0	0	0	0	7	0	0	0	6
hellaswag	11	0	0	13	0	2	0	0	0	0	3
pubmedqa	11	0	0	8	0	0	6	4	0	0	9
sciq	11	0	0	0	0	0	16	0	2	10	14
triviaQA	11	0	0	0	60	17	0	0	3	0	20
wikitext	11	0	38	11	0	10	0	0	8	0	22
truthfulQA	11	100	62	48	12	71	50	0	84	0	18
LLM Performance	47	52	53	54	48	57	51	58	60(*)	40	51

1401
1402
1403

In the table below (for clarity reasons, the numbers are rounded), we show the data mixing ratio found by DUET-IF at each iteration as compared to that found by DoReMi for the in-domain TruthfulQA task in **Fig. 4(a)** (to bridge the discussion point we raised above). We also show the data mixing ratio found by DoReMi.

1404 We used a uniform data mixture ($\sim 11\%$ of data to each data domain) as the initial data mixture for
1405 BO. By chance (since BO with a confidence-based acquisition function tends to explore boundary
1406 inputs initially), it finds that placing more emphasis on the TruthfulQA data domain yields better
1407 LLM performance. After some adjustments, in the 9th iteration, the best performing data mixture
1408 was found. In fact, in some of our exploratory process, we found that if we increased the number
1409 of iterations beyond 10, we can find even better training data mixtures, but the gain in performance
1410 typically plateaus (as in many BO applications).

1411 **Comparison to DoReMi:** We can see that DoReMi adopts a distributionally robust approach and
1412 allocates mixture weights more uniformly across different domains (since it cannot exploit the task
1413 feedback to infer that truthfulQA data is more relevant). This is clearly suboptimal because it is not
1414 optimized specifically towards the evaluation task. and hence its data mixture does not perform as
1415 well as DUET-IF, as shown in our experiments.

1416
1417
1418
1419
1420
1421
1422
1423
1424
1425
1426
1427
1428
1429
1430
1431
1432
1433
1434
1435
1436
1437
1438
1439
1440
1441
1442
1443
1444
1445
1446
1447
1448
1449
1450
1451
1452
1453
1454
1455
1456
1457